國立交通大學

電信工程研究所

碩 士 論 文

使用雙極化天線的空間調變技術：
訊號映射、通道估測及訊號偵測

Spatial Modulation Using Dual-Polarized Antennas:
Signal Mapping, Channel Estimation and Data Detection

研 究 生：林可涓

指導教授：蘇育德　教授

中 華 民 國 一百零一 年 七 月

使用雙極化天線的空間調變技術：
訊號映射、通道估測及訊號偵測

Spatial Modulation Using Dual-Polarized Antennas: Signal Mapping, Channel Estimation and Data Detection

研 究 生：林可涓　　Student：Ke-Jyuan Lin

指導教授：蘇育德　　Advisor：Dr. Yu T. Su

國 立 交 通 大 學

電信工程研究所

碩 士 論 文

A Thesis

Submitted to the Institute of Communications Engineering

in partial Fulfillment of the requirements

for the Degree of

Master of Science

in

Communications Engineering

at the

National Chiao Tung University

July 2012

Hsinchu, Taiwan, Republic of China

公元 2012 年七月

使用雙極化天線的空間調變技術：訊號映射、通道估測及訊號偵測

學生：林可涓　　指導教授：蘇育德

國立交通大學電信工程研究所碩士班

摘　　要

空間調變 (SM) 是近年來被提出的一種提升頻譜效率及降低傳送接收端複雜度的技術。 這是由於 SM 可避免傳統 MIMO 技術中通道間交互干擾 (ICI) 的問題，且大量減少硬體上射頻鏈路 (RF chain) 的高花費。

大多數對於 MIMO 訊號的偵測，傳送或是接收端需要知道通道資訊 (CSI)，此通道資訊可透過某種估計演法得到。在本文中，提出了兩種基於 SM 系統下，隨時間變動的通道估測方法，此方法可以省掉領航信號 (pilot) 的額外負擔因此而提升系統效能。

因為共置 (co-located) 雙極化天線的使用可以節省空間和花費，因此我們也探討使用雙極化天線的SM技術及其訊號偵測的方法，其中所提出的次佳化的偵測器複雜度只需要將近最大似然偵測法 (ML) 的一半，且效果比基於匹配濾波器 (MF-based) 的偵測法更好。在使用雙極化天線及有空間相關性的通道模型中，我們也引進了一個較一般性的通道模型並提出相對應的通道估測方法。

由於 SM 系統在傳送訊號時，一次只使用單根傳送天線，利用 Alamouti 的時空編碼可以使 SM 系統更具彈性。本文中提出了在 SM 系統下差分的 Alamouti 時空編碼技術，此法接收端不須要通道資訊即可解碼。

針對所提出的方法，我們透過了模擬結果來檢驗其效能並與現有的方法做比較。

Spatial Modulation Using Dual-Polarized Antennas: Signal Mapping, Channel Estimation and Data Detection

Student : Ke-Jyuan Lin Advisor : Yu T. Su

Institute of Communications Engineering

National Chiao Tung University

Abstract

Spatial modulation (SM) technique has received intensive interest recently for its capability to improve the spectral efficiency and lower the transceiver complexity. This is because SM induces zero inter-channel interference and requires a single RF chain only.

To detect or encode SM signals, channel state information (CSI), which is to be obtained by a channel estimator at either the transmit or the receive side, is needed for spatial identification. The first SM-related issue investigated in this thesis concerns channel estimation in a correlated time-varying channel. We propose superimposed-pilot-assisted and decision-directed spatial channel estimation schemes. These schemes improve the system throughput by either removing or reducing the pilot overhead.

Since the use of co-located dual-polarized antennas offers a space- and cost-effective alternative for multiple antenna systems, we then review the feasibility of using such antenna arrays and present a new SM scheme which takes advantage of the channel decorrelation inherited in a dual-polarized antenna array. A suboptimal detector which needs only half of the ML detector complexity is proposed. This suboptimal detector performs much better than the MF-based method. For a dual-polarized antenna array

based SM system, we suggest a general channel model which takes into account the spatial correlation and introduce a model-based spatial channel estimator.

Finally, to avoid the CSI requirement, we propose an Alamouti coding based differential space time block coded SM (DSTBC-SM) scheme.

For each proposed scheme, we provide computer simulation results to demonstrate and verify its superiority against the existing solutions.

誌　　謝

對於論文得以順利完成，首先感謝指導教授 蘇育德博士。老師的教誨使我對於通訊領域的研究有更深入的了解，也教導我們許多書上學不到的知識與人生道理，讓我受益匪淺。並感謝口試委員蘇賜麟教授、林茂昭教授及呂忠津教授給予的許多意見，以補足這份論文的缺失與不足之處。

我也非常感謝實驗室的劉彥成學長，在我研究上有問題時，能給予我建議及討論，使我的研究能夠順利完成，從中學習到的經驗是很珍貴的。另外也感謝實驗的成員們，在這兩年內的互相支持與鼓勵。

最後，要感謝我的家人及朋友，他們總是在背後默默的關心與支持，使我有動力可以努力往前進，在此僅獻上此論文，以代表我最深的敬意。

Contents

List of Tables

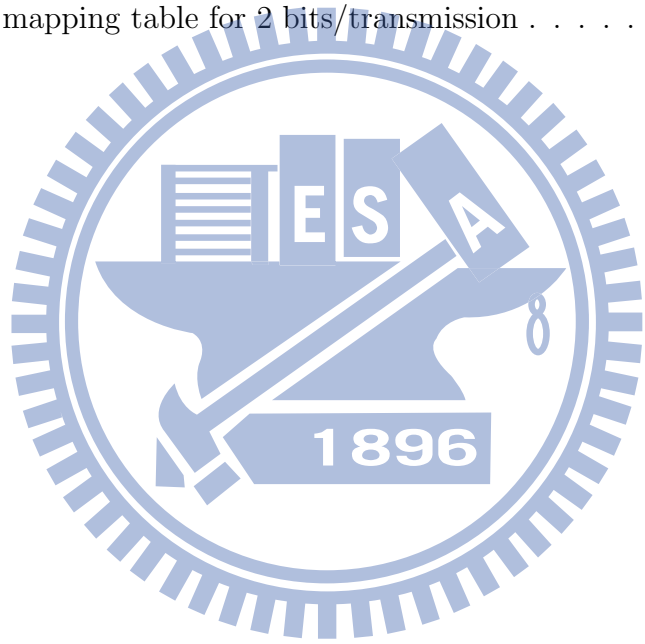

List of Figures

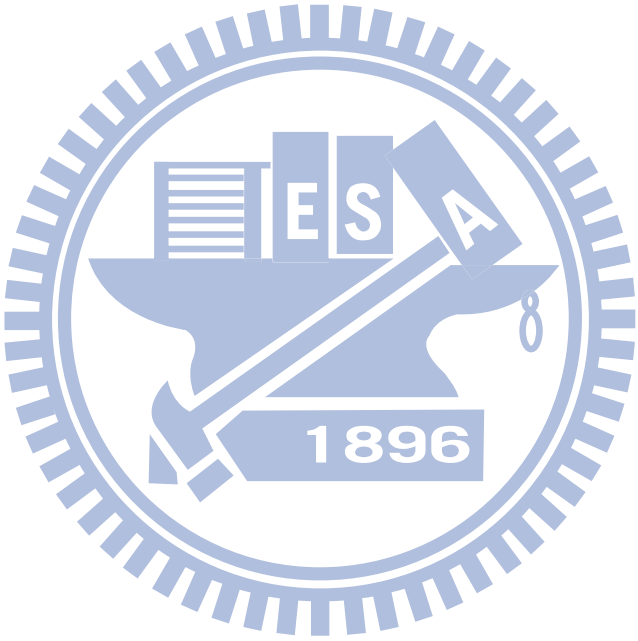

Chapter 1

Introduction

Multiple-input and multiple-output (MIMO) techniques have drawn intensive attention and R&D efforts in the past decade as they promise to offer a system capacity which is linearly proportional to the minimum of the transmit and receive antennas numbers [1]-[3] in a richly scattered environment. The extra spatial degrees of freedom is specially welcome for wireless communication system designers who are always looking for novel transmission techniques to achieve both high data rate and high spectral efficiency.

Many existing techniques have been developed to exploit the promised MIMO capacity. One simple yet efficient scheme to achieve the full diversity (array) gain is the class of space-time codes (STC) [4]. Besides achieving full diversity gain with low receiver complexity, it also has high spectral efficiency of one symbol per channel use [5]. The Bell Labs layered space-time (BLAST) [6], on the other hand, demultiplexes data streams into a number of substreams which are then transmitted by different antennas, resulting in a data rate increase proportional to the number of transmit antennas. The multiplexing gain, however, is obtained by using equal number of receive antennas and complex signal processing at the receive side to eliminate the inter-(spatial)channel interference (ICI).

Another transmission technique which uses multiple antennas is spatial modulation (SM). SM is a simple scheme which avoids ICI, timing synchronization of multiple spatial data streams and reduces the cost of multiple radio frequency (RF) chains by allowing

one transmit (and receive) antenna to be active in any one transmission interval [7]. In addition, SM can exploit transmit antenna index to convey information to enhance spectral efficiency and capacity [11]. The low system complexity requirement, relative high spectral efficiency, and robust error performance in correlated channels [8] have made SM an attractive candidate for high rate transmissions. However, the SM system needs at least two transmit antennas and the transmit-receive wireless links have to be sufficiently dissimilar to each other to yield adequate performance [9]. When the only information is carried by the transmit antenna index, SM degenerates to the so-called space shift keying (SSK) modulation [10] which is easy to implement although the associated achievable data rate is rather limited.

Maximum likelihood (ML), matched-filter (MF)-based and sphere detection (SD) based receivers have been introduced for detecting SM signals [12], [13]. These detectors perform fairly well only when the channel state information (CSI) is perfectly known by the receiver. CSI is often obtained by using a pilot-assisted least square (LS) or minimum mean square error (MMSE) channel estimator [14]. In most cases, the channel is assumed to be either static (time-invariant) or block faded [15], [16], these known estimators yield poor performance valid for time-varying or correlated block-fading channels. In this thesis, we propose two channel estimation schemes for use in time-varying block-faded channels that takes advantage of the SM structure. The first scheme is a decision-directed one which uses the detected signals of previous blocks to update estimated channel coefficients. Since the selected transmit antenna is uniformly distributed, all CSIs would be updated in a sufficient long transmission period. The performance of this scheme has error floor in high SNR (signal-to-noise ratio) region due to the propagation of channel estimation error. We introduce a superimposed pilot CSI estimation scheme to overcome this shortcoming and improve the system performance without incurring extra pilot overhead.

While multiple spatially-separated antennas at the transmitter and receiver can pro-

vide multiplexing and/or array gains, these antennas need to have a large physical separation to yield uncorrelated spatial channels. A space- and cost-effective alternative [17] can be obtained by using co-located orthogonally-polarized antennas. A MIMO channel using dual polarized antennas has a better channel condition as compared to that of the conventional one when fixing antenna numbers and the area that can accommodate antenna hardware. Moreover, the use of such antennas offers additional degree of freedom with the same structure of antenna array [18]. The dual-polarized antenna system, however, possesses complicated depolarized properties because of the coupling effect between different orthogonal polarizations as were shown in [19], [20], [21]; measurements of depolarization parameters can be found in [19].

We make use of the advantages inherited in dual-polarized antennas and propose a new scheme called dual-polarized spatial modulation (DPSM) to fully exploit multi antenna capabilities. This scheme convey information in the polarization of antenna, antenna index, and symbol transmitted. It can outperform conventional MIMO system in correlated channel because of the better channel condition. Moreover, we develop the ML detector and the MF-based detector of DPSM, and we propose a sub-optimal DPSM detector whose complexity is almost half of ML detector and its performance is much better than MF-based method. In addition, DPSM assuages the problem of poor SM performance when the transmit-to-receive wireless links are too much alike, i.e., the MIMO channel is too correlated or has a bad condition [9].

Spatial correlation is also considered in dual-polarized channels. In [19], [21], [22] the transmit and receive spatial correlations are assumed to be de-coupled, resulting in Kronecker-like model [23]. As spatial correlation between transmitter and receiver does exist [24], alternate correlated channel models are introduced to incorporate this joint correlation [25], [26]. However, these analytic models often call for the knowledge of second-order channel statistics that are not easy to obtain, [27] proposed a reduced-rank channel model and compact CSI representation to solve this inconvenience. and

generalizes the above-mentioned channel models. In this thesis, we combine this model with dual-polarization effects and propose a modified channel estimation method for this modified dual-polarized channel model.

Finally, we notice that space-time block-coded spatial modulation (STBC-SM) has been proposed recently [28] to improve the SM spectral efficiency. An Alamouti coded-based differential STBC-SM (DSTBC-SM), which dose not need CSI and performs well in slow time-varying channel, is studied.

The rest of this thesis is organized as follows. In Chapter 2 we present the transceiver structure of a typical SM system along with spatial correlated channel models. In Chapter 3, we propose two time varying channel estimation methods for SM systems and give simulated performance. Chapter 4 describes a dual-polarized antenna array based SM scheme and the associated CSI estimation methods for spatial correlated channels. Space-time-coded systems are introduced in Chapter 5. Our main contributions are summarized in Chapter 6.

The following notations are used throughout the thesis: upper case bold symbols denote matrices and lower case bold symbols denote vectors. $\mathbf{I}_N$ is a $N \times N$ identity matrix. $(\cdot)^T, (\cdot)^H$, and $(\cdot)^\dagger$ represent the transpose, conjugate transpose, and pseudo-inverse of the enclosed items, respectively. $(\cdot)^{-1}$ denotes the inverse of matrix. $vec(\cdot)$ is the operator that forms one tall vector by stacking columns of a matrix. While $\mathbb{E}\{\cdot\}$, $|\cdot|$, and $\|\cdot\|_F$ denote the expectation, absolute value, and Frobenius norm of the enclosed items, respectively, $\odot$ and $\otimes$ are respectively the Hadamard and Kronecker product.

Chapter 2

Preliminaries

2.1 Conventional MIMO System Model

When MIMO system is used in wireless communications, it is commonly referred to the uni-polarized multiple input multiple out antenna system. These antennas are spatial separated to yield an uncorrelated channel, thus they can provide diversity gain and increase the reliability of wireless links [1]. Moreover, under suitable channel fading conditions, spatially multiplexing gain can be achieved and increase the MIMO capacity.

For conventional MIMO system, the MIMO channel between transmitter and receiver at time k is modeled as

$$\mathbf{H}(k,\tau) = \sum_{p=1}^{G} \mathbf{H}_p(k)\delta(t-\tau_p), \tag{2.1}$$

where G is the maximum number of paths between the subchannel of a transmit and receive antenna pair. τ_p is the delay of the pth path , and δ denotes the Dirac delta function. If we consider a narrowband flat-fading MIMO system with N_T transmit antennas and N_R receive antennas, MIMO channel representation is reduced to a $N_R \times N_T$ single-tap fading channel matrix. Then when data vector $\mathbf{x}(t)$ is transmitted, the received signal is denoted as

$$\mathbf{y}(k) = \mathbf{H}(k)\mathbf{x}(k) + \mathbf{z}(k), \tag{2.2}$$

where for rayleigh-fading spatial-uncorrelated channel, the elements of $\mathbf{H}(k)$ are independent and identically distributed, zero mean complex Gaussian random variables. $\mathbf{z}(k)$ is the additive white Gaussian noise (AWGN) vector, whose entries are of zero mean and with variance σ_z^2. Figure 2.1 gives the brief MIMO system model,

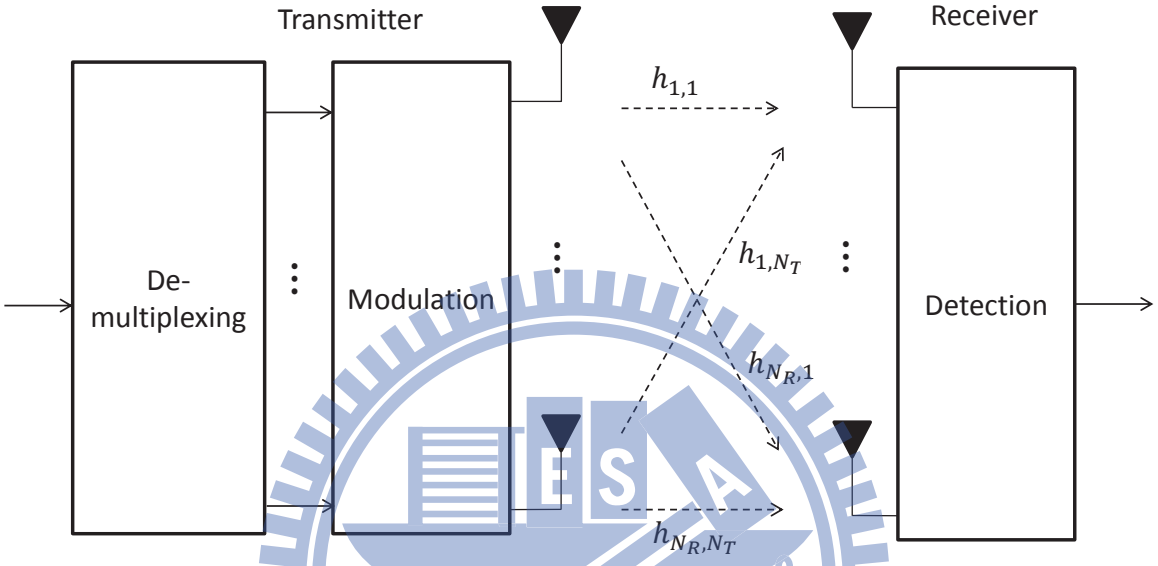

Figure 2.1: A MIMO system model.

2.2 Spatial Modulation (SM) Schemes and Their Detections

In MIMO system, many transmission techniques have been designed to improve spectral efficiency such as vertical Bell Laboratories layered space-time (V-BLAST) architecture. BLAST transmission systems suffer from high inter-channel interference resulting from the simultaneous transmissions on the same frequency for MIMO channel. Spatial modulation (SM) is an innovative approach which can boost the spectral efficiency and further avoid ICI by using active transmit antenna indices as additional source of information. In the following subsections, we will discuss the transceiver design of SM.

2.2.1 Spatial Modulation Transmission

We consider the block fading case that channel gain remains unchanged within a block time and eliminate the time parameter t in this chapter. To begin with, data bits are partitioned into groups of $m = \log_2(MN_T)$ bits where in each group the first $\log_2 N_T$ bits indicate the transmit antenna to be used and the remaining bits corresponds to an M-QAM symbol. This M-QAM constellation is denoted as $\mathcal{A}_M$ and the symbol in it are transmitted by the indexed antennas. Figure 2.2 depicts the system model described above.

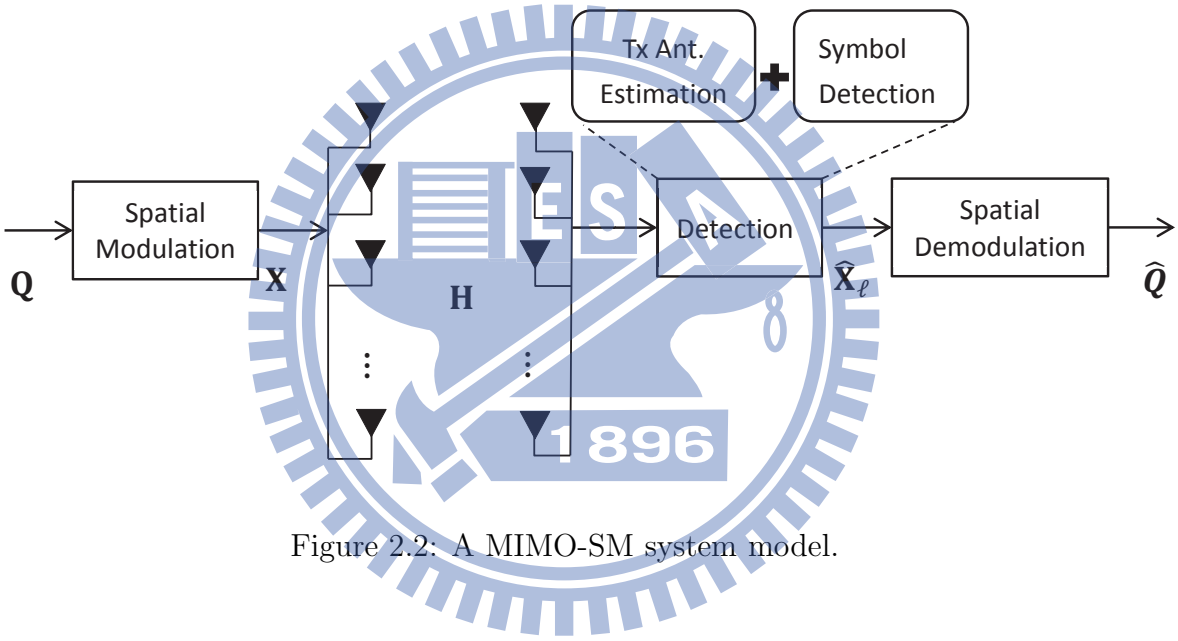

Figure 2.2: A MIMO-SM system model.

Spatial modulation (SM) maps $m \times B$ data matrix $\mathbf{Q}$ to $\mathbf{X}$, $N_T \times B$ transmitted signal matrix, where B denotes block size which should be equal or larger than N_R. The reason is that Matrix $\mathbf{X} \triangleq [\mathbf{x}_1, \cdots \mathbf{x}_B]$ has only one nonzero element in each column where $\mathbf{x}_i$ is the signal vector transmitted at the ith time slot. At time slot i, the ℓth entry of $\mathbf{x}_i$, $x_{\ell,i}$, is the transmit symbol of antenna ℓ. The case when $x_{\ell i} = 0$ means antenna ℓ is not used at the ith instant. One example of SM mapping rule is shown in Table 2.1.

Input bits	Antenna Index	Transmit Symbol		Antenna Index	Transmit Symbol
000	1	+1		1	+1 + j
001	1	-1		1	-1 + j
010	2	+1		1	-1 - j
011	2	-1		1	+1 - j
100	3	+1		2	+1 + j
101	3	-1		2	-1 + j
110	4	+1		2	-1 - j
111	4	-1		2	+1 - j

Table 2.1: SM mapping table for 3 bits/transmission

At the receiver side, the $N_R \times B$ received signal matrix $\mathbf{Y}$ can be expressed as

$$\mathbf{Y} = \mathbf{H}\mathbf{X} + \mathbf{Z}, \tag{2.3}$$

where

$$\mathbf{X} = [\mathbf{x}_1, \cdots, \mathbf{x}_B]; \tag{2.4}$$

$$\mathbf{Y} = [\mathbf{y}_1, \cdots, \mathbf{y}_B]; \tag{2.5}$$

$$\mathbf{Z} = [\mathbf{z}_1, \cdots, \mathbf{z}_B]; \tag{2.6}$$

$$\mathbf{H} = [\mathbf{h}_1, \cdots, \mathbf{h}_{N_T}]. \tag{2.7}$$

Matrix $\mathbf{H}$ describes the overall $N_R \times N_T$ channel matrix whose (m, n)-th element $h_{m,n}$ is the channel response between the nth transmit antenna and the mth receive antenna. The elements of $\mathbf{H}$ are independent and identically distributed (i.i.d.), zero-mean complex Gaussian random variables with unit variance, $\sigma_h^2 = 1$. In addition, $\mathbf{Z}$ is the $N_R \times B$ additive white Gaussian noise (AWGN) matrix, whose entries are of zero mean and $\mathbb{E}\{\, \mathbf{z}_i\, \mathbf{z}_i^H \} = \sigma_z^2\, \mathbf{I}_{N_R}$, observed at the receiver. We assume an average transmit power of E_x, i.e.,

$$\mathrm{E}_x = \frac{1}{B}\, \mathbb{E}\,[\, \|\, \mathbf{X}\, \|_F^2\,] = \frac{1}{B}\, \mathbb{E}\,[\, tr\, \{\, \mathbf{X}\mathbf{X}^H \}\,], \tag{2.8}$$

Through this thesis, we consider a quasi-static scenario, where channel remains unchanged over the period of B and is independent of both $\mathbf{X}$ and $\mathbf{Z}$.

Because only one transmit antenna is active, say ℓth antenna, during symbol time i, alternatively we have

$$\mathbf{y}_i = \mathbf{h}_\ell x_{\ell i} + \mathbf{z}_i, \tag{2.9}$$

where $x_{\ell i} \in \mathcal{A}_M$ and for $i = 1, \cdots, B$, $i = 1, \cdots, N_T$

$$\mathbf{x}_i = [0, \cdots, x_{\ell,i}, \cdots, 0]^T \in \mathcal{C}_{N_T}, \tag{2.10}$$

$$\mathbf{y}_i = [y_{1,i}, \cdots, y_{N_R,i}]^T \in \mathcal{C}^{N_R}, \tag{2.11}$$

$$\mathbf{z}_i = [z_{1,i}, \cdots, z_{N_R,i}]^T \in \mathcal{C}^{N_R}, \tag{2.12}$$

$$\mathbf{h}_j = [h_{1,j}, \cdots, h_{N_R,j}]^T \in \mathcal{C}^{N_R}. \tag{2.13}$$

2.2.2 Optimal Detector

Due to SM's specific structure, its receiver is inherently of low complexity. With the assumption that the channel state information (CSI) $\mathbf{H}$ is known to the receivers, we introduce the single-stream-based maximum likelihood (ML) and matched filter (MF)-based detector respectively in this and the next subsection, respectively.

Since the channel coefficients are assumed equally likely, the optimal detector based on the ML principle is equal to maximizing the probability $P(\mathbf{Y}|\mathbf{H}, \mathbf{X})$ [29],

$$P(\mathbf{Y}|\mathbf{H}, \mathbf{X}) = \frac{1}{(\pi\sigma_z^2)^{N_R}} e^{-\frac{1}{\sigma_z^2}\|\mathbf{Y}-\mathbf{H}\mathbf{X}\|_F^2}. \tag{2.14}$$

ML detection exhaustively searches over all transmit antenna index and constellation point pairs. It is often regarded as a high complexity detection technique. However, the complexity of SM's ML detector is much reduced due to the fact that only one transmit antenna is used at a time. Therefore, the ML metric of each time can be expressed as

$$(\hat{\ell}_i, \hat{x}_{\ell i}) = \arg\max_{\ell, x_{\ell i}} P(\mathbf{y}_i|\mathbf{H}, \mathbf{x}_i) = \arg\min_{\ell, x_{\ell i}} \|\mathbf{y}_i - x_{\ell i}\mathbf{h}_\ell\|^2, \tag{2.15}$$

whose search space is of order $O(MN_T)$. It is also called the single-stream-based ML detector

2.2.3 Sub-Optimal Detector

For the MF-based detector, we need to normalize every column of $\mathbf{H}$ by its norm before estimation of transmit antenna index. The reason is as follows. First, let

$$\bar{\mathbf{h}}_j = \frac{\mathbf{h}_j}{\|\mathbf{h}_j\|},\ j = 1, \cdots, N_T. \tag{2.16}$$

As Cauchy-Schwarz inequality suggests:

$$|\bar{\mathbf{h}}_\ell^H \mathbf{h}_\ell| = \|\mathbf{h}_\ell\| = \frac{\|\mathbf{h}_j\|\|\mathbf{h}_\ell\|}{\|\mathbf{h}_j\|} \geq |\bar{\mathbf{h}}_j^H \mathbf{h}_\ell|,\ \ell = 1, \cdots, N_T, \tag{2.17}$$

we can define the MF receiver as

$$\mathbf{g}_j = \bar{\mathbf{h}}_j^H \mathbf{y}_i,\ i = 1, \cdots, B, \tag{2.18}$$

which reduces to $\|\mathbf{h}_\ell\| x_{\ell,i}$ plus noise if $j = \ell$ or noise only when $\mathbf{y}_i = x_{\ell i}\mathbf{h}_\ell + \mathbf{z}_i$. Therefore, we can estimate transmit antenna index by finding the maximum value of $|g_j|$.

$$\hat{\ell}_i = \underset{\ell_i \in \{1, \cdots, N_T\}}{\arg\max}\ |g_{\ell_i,i}|. \tag{2.19}$$

Next, left-multiplying $\mathbf{y}_i$ by the pseudo-inverse of $\mathbf{h}_{\hat{\ell}_i}$ ($\mathbf{h}_{\hat{\ell}_i}^\dagger = (\mathbf{h}_{\hat{\ell}_i}^H \mathbf{h}_{\hat{\ell}_i})^{-1}\mathbf{h}_{\hat{\ell}_i}^H$) and quantizing this product to the constellation points with function $Q(\cdot)$ to recover transmit symbol $\hat{x}_{\hat{\ell}_i,i}$, i.e.,

$$\check{g}_{\hat{\ell}_i,i} = \mathbf{h}_{\hat{\ell}_i}^\dagger \mathbf{y}_i = \frac{\mathbf{h}_{\hat{\ell}_i}^H \mathbf{y}_i}{\|\mathbf{h}_{\hat{\ell}_i}\|^2} = \frac{g_{\hat{\ell}_i,i}}{\|\mathbf{h}_{\hat{\ell}_i}\|}, \tag{2.20}$$

$$\hat{x}_{\hat{\ell}_i,i} = Q(\check{g}_{\hat{\ell}_i,i}). \tag{2.21}$$

2.3 Spatial-Correlated MIMO Channel Models

2.3.1 Conventional Correlated Channel Model

In general, a full correlation matrix $\mathbf{R}$ that specifies the $N_R N_T \times N_R N_T$ mutual correlation coefficients between all channel matrix elements is used to describe the spatial behavior of a general MIMO channel; specifically,

$$\mathbf{R} \triangleq \mathbb{E}\{vec(\mathbf{H}^H)vec(\mathbf{H}^H)^H\}. \tag{2.22}$$

For example, the spatial correlation matrix of a 2×2 MIMO channel can be described as

$$\mathbf{R} = \begin{bmatrix} 1 & t^* & r^* & s_1^* \\ t & 1 & s_2^* & r^* \\ r & s_2 & 1 & t^* \\ s_1 & r & t & 1 \end{bmatrix}, \tag{2.23}$$

where t and r are transmit and receive antenna correlation coefficients, and $s_1 \overset{\text{def}}{=} \mathbb{E}\{h_{1,1}h_{2,2}^*\}$ and $s_2 \overset{\text{def}}{=} \mathbb{E}\{h_{1,2}h_{2,1}^*\}$ are cross-channel correlation coefficients.

Consequently, a spatial correlated Rayleigh fading channel can be modeled as

$$vec(\mathbf{H}^H) = \mathbf{R}^{\frac{1}{2}} vec(\mathbf{H}_\omega^H), \tag{2.24}$$

where $\mathbf{H}_\omega$ is the i.i.d. complex Gaussian matrix with unit variance.

However, there are some difficulties in using this model. First, large number of transmit and receive antennas will make the number of correlation matrix elements, $(N_R N_T)^2$, too large to compute. Moreover, physical propagation of the radio channel, such as angle of arrival (AOA), direction of departure (DOD), and etc., could not be easily interpreted by this correlation matrix [24].

2.3.2 Kronecker Model

Kronecker model is commonly used when correlation between transmit and receive antennas are independent and can be separated that the spatial correlation matrix is given by the Kronecker product of those of the transmit and receive antennas, which is reasonable when the main scattering is locally rich at each transmitter and receiver side

[24],

$$\mathbf{H} = \mathbf{R}_R^{\frac{1}{2}} \mathbf{H}_\omega (\mathbf{R}_T^{\frac{1}{2}})^T, \tag{2.25}$$

where $N_T \times N_T$ matrix $\mathbf{R}_T$ and $N_R \times N_R$ $\mathbf{R}_R$ represent spatial correlation of transmit and receive antennas, respectively.

The separation statistic of Kronecker model implies that $N_R N_T \times N_R N_T$ correlation matrix of $\mathbf{H}$ can be expressed as

$$\mathbf{R} = \mathbf{R}_R \otimes \mathbf{R}_T. \tag{2.26}$$

Since the strict assumption of separate correlation between transmitter and receiver side, it would not be appropriate to model a correlated channel where transmitter and receiver side have some correlation leading to capacity and error probability misfits.

2.3.3 Virtual Channel Representation and Weichselberger Model

Both [25] and [26] consider joint correlation at both ends of MIMO channel, so the correlated channel is modeled by basis matrices of two one-sided correlation matrix and one coupling matrix which contains the correlation between transmitter and receiver side. In [25], a virtual channel representation using predefined discrete Fourier transform (DFT) matrices is proposed to model the correlated channel. Specifically,

$$\mathbf{H} = \mathbf{F}_R (\tilde{\mathbf{\Omega}}_{virt} \odot \mathbf{H}_\omega) \mathbf{F}_T^H, \tag{2.27}$$

where $\mathbf{F}_R$ and $\mathbf{F}_T$ are respectively $N_R \times N_R$ and $N_T \times N_T$ are predefined DFT matrices and $\tilde{\mathbf{\Omega}}_{virt}$ is the coupling matrix. However, this model is restricted to single polarized uniform linear arrays (ULAs) only, we therefor introduce in the following a model that copes with this issue.

In [26], eigenbases of transmit and receive correlation matrices are used to model this spatial correlated channel, i.e.,

$$\mathbf{H} = \mathbf{U}_R (\tilde{\mathbf{\Omega}} \odot \mathbf{H}_\omega) \mathbf{U}_T^H, \tag{2.28}$$

where $\mathbf{U}_R$ and $\mathbf{U}_T$ are the eigenbasis of the receive and transmit correlation matrix, respectively. With $\mathbf{\Lambda}_R$ and $\mathbf{\Lambda}_T$ being the diagonal matrices comprise the eigenvalues, which are nonnegative, of $\mathbf{R}_R$ and $\mathbf{R}_T$, the eigen decompositions of $\mathbf{R}_R$ and $\mathbf{R}_T$ are

$$\mathbf{R}_R = \mathbf{U}_R \mathbf{\Lambda}_R \mathbf{U}_R^H \quad \text{and} \quad \mathbf{R}_T = \mathbf{U}_T \mathbf{\Lambda}_T \mathbf{U}_T^H, \tag{2.29}$$

$\tilde{\mathbf{\Omega}}$ is the element-wise square root of the coupling matrix $\mathbf{\Omega}$ which is defined as

$$[\mathbf{\Omega}]_{i,j} = \mathbb{E}\{|\mathbf{u}_{R,i}^H \mathbf{H} \mathbf{u}_{T,j}^*|^2\}, \ i = 1, \ldots, N_R, j = 1, \ldots, N_T. \tag{2.30}$$

where $\mathbf{u}_{R,i}$ and $\mathbf{u}_{T,j}$ are the ith and jth column vector of $\mathbf{U}_R$ and $\mathbf{U}_T$, respectively. From this coupling matrix, the mean amount of energy that is coupled with an eigenvector of one side to that of the other can be identified a more general framework of channel model.

2.3.4 Model-Based Correlated Channel

The model-based correlated channel is introduced by [27]. Since the channel matrix $\mathbf{H}$ can be decomposed via singular value decomposition (SVD), $\mathbf{H} = \mathbf{U}\mathbf{\Lambda}\mathbf{V}^H$, where $\mathbf{U}$ and $\mathbf{V}$ are $N_R \times N_R$ and $N_T \times N_T$ unitary matrices, respectively, and $\mathbf{\Lambda}$ is a $N_R \times N_T$ diagonal matrix with non-negative entries. The two unitary matrices can be represented by predefined unitary matrices $\mathbf{Q}_1$ and $\mathbf{Q}_2$ as $\mathbf{U}\mathbf{P}_1 = \mathbf{Q}_1$ and $\mathbf{V}\mathbf{P}_2 = \mathbf{Q}_2$ where $\mathbf{P}_1$ and $\mathbf{P}_2$ are unitary. As a result, we have

$$\mathbf{H} = \mathbf{Q}_1 \mathbf{P}_1^{-1} \mathbf{\Lambda} (\mathbf{P}_2^{-1})^H \mathbf{Q}_2^H = \mathbf{Q}_1 \mathbf{C} \mathbf{Q}_2^H, \tag{2.31}$$

where $\mathbf{C}$ is a complex random matrix, equation (2.29) can be regarded as a generalization of all the models mentioned above. To be specific, it is equivalent to the Kronecker model if $\mathbf{C}$ satisfies

$$vec(\mathbf{C}) = (\mathbf{\Xi}_T \otimes \mathbf{\Xi}_R) vec(\mathbf{H}_\omega), \tag{2.32}$$

where $\mathbf{\Xi}_T$ and $\mathbf{\Xi}_R$ are obtained by Gram-Schmidt orthonormalization with $\mathbf{R}_T^{\frac{1}{2}} = \mathbf{Q}_2 \mathbf{\Xi}_T$ and $\mathbf{R}_R^{\frac{1}{2}} = \mathbf{Q}_1 \mathbf{\Xi}_R$, and is related to the Weichselberger model when

$$\mathbf{U}_T = \mathbf{Q}_2 \mathbf{P}_T^H \quad \text{and} \quad \mathbf{U}_R = \mathbf{Q}_1 \mathbf{P}_R^H, \tag{2.33}$$

with $\mathbf{P}_T$ and $\mathbf{P}_R$ being the eigenbasis matrices of $\mathbb{E}\{\mathbf{C}\mathbf{C}^H\}$ and $\mathbb{E}\{\mathbf{C}^T\mathbf{C}^*\}$ whose eigenvalues are the same as those of $\mathbb{E}\{\mathbf{H}\mathbf{H}^H\}$ and $\mathbb{E}\{\mathbf{H}^T\mathbf{H}^*\}$. Finally, if $\mathbf{Q}_1$ and $\mathbf{Q}_2$ are chosen to be composed of columns of DFT matrices, this general model is compatible with the virtual channel representation by Sayeed [25].

The fact that second-order statistics is not required, because spatial correlation is captured by predetermined nonparametric regression, reduces the number of parameters needed to be estimated when modelling the channel $\mathbf{H}$ by (2.29). This provides a great complexity reduction when the dimension of $\mathbf{H}$ is large.

Chapter 3

Estimation of Spatial-Modulated Time-Varying Channels

In this chapter, we first give a review of conventional pilot-based channel estimation techniques and present the proposed time-varying channel estimation methods for SM system.

3.1 Conventional Pilot-Based Channel Estimation Methods

Considering a time-varying block-fading channel, its CSI is obtained by transmitting pilot signal which is known to the receiver. Assume pilot signal matrices $\mathbf{X}_P(k)$'s are of size $N_T \times B$ and the average pilot symbol energy equals to the data symbol energy. The received signal at kth block time can be written as

$$\mathbf{Y}_P(k) = \mathbf{H}(k)\mathbf{X}_P(k) + \mathbf{Z}_P(k), \tag{3.1}$$

where $\mathbf{Y}_P(k)$ is $N_R \times B$. $\mathbf{H}(k)$ is the $N_R \times N_T$ MIMO channel matrix at time k, and the entries of AWGN matrix $\mathbf{Z}_p(k)$ are i.i.d., zero mean complex Gaussian with variance σ_z^2.

To estimate a time-varying channel, pilot signal blocks are inserted in transmit data stream periodically. Transmit data detection can thus be conducted with the estimated channel. However, if the channel changes rapidly, the period of pilot signal insertion

should be short to keep up with the change. This in turn reduces the power or spectral efficiency of the data signal. We illustrate this idea in Figure 3.1.

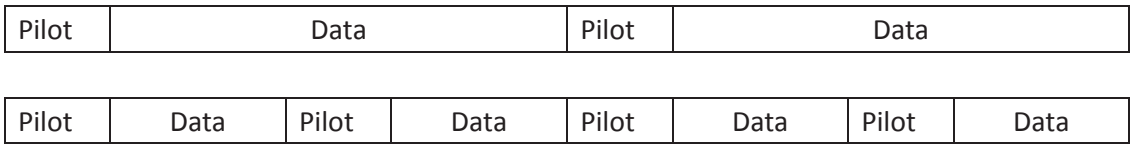

Figure 3.1: Periodical pilot signal insertion in transmit data.

Two conventional pilot-based channel estimation methods which are discussed in the following.

3.1.1 Least Square Channel Estimation

The least square (LS) channel estimate of $\mathbf{H}(k)$ is found by minimizing the squared error $\|\mathbf{Y}_P(k) - \mathbf{H}(k)\mathbf{X}_P(k)\|^2$ [29]. As a result, the estimated channel $\hat{\mathbf{H}}_{LS}(k)$ can be derived by

$$\begin{aligned} \hat{\mathbf{H}}_{LS}(k) &= \mathbf{Y}_P(k)\mathbf{X}_P^H(k)(\mathbf{X}_P(k)\mathbf{X}_P^H(k))^{-1} \\ &= \mathbf{H}(k) + \mathbf{Z}_P(k)\mathbf{X}_P^H(k)(\mathbf{X}_P(k)\mathbf{X}_P^H(k))^{-1}. \end{aligned} \tag{3.2}$$

While the main advantage of the LS channel estimation method is its low complexity, it fails to take the statistics of the channel and noise into account. Such obliviousness can result in significant noise power enhancement offer channel equalization performance degradation. As LS estimation may be a suitable solution when channel and noise statistics are unknown, it is not sufficient for our requirement.

3.1.2 Minimum Mean Square Error Channel Estimation

In order to solve the noise enhancement problem, minimum mean square error (MMSE) channel estimation method is introduced. As its name suggests, if $\mathbf{F}$ minimizes

the mean square error $\mathbb{E}\{\|\mathbf{Y}_P(k)\mathbf{F}-\mathbf{H}(k)\|^2\}$. Since the entries of $\mathbf{H}(k)$ are assumed to be unit-variance, we have

$$\hat{\mathbf{H}}_{MMSE}(k) = \mathbf{Y}_P(k)\mathbf{X}_P^H(k)(\sigma_z^2\mathbf{I}_{N_T} + \mathbf{X}_P(k)\mathbf{X}_P^H(k))^{-1} \tag{3.3}$$

Based on the abovementioned channel estimation methods, we propose two time-varying channel estimation methods for SM systems and discuss in the ensuing sections.

3.2 Decision-Directed SM Channel Estimation

The main idea of decision-directed channel estimation is to track channel variations using detected data symbols of previous blocks as pilots. This method saves the pilot signal overhead and thus retains the data rate. Due to the SM systems' capability to avoid ICI, the utilization of detected data symbols can be a good approach to estimate channel. The reason is that it is proved the optimal channel estimation performance can be achieved by using unitary pilot signal matrices which help decoupling channel vectors at the receiver [30], [31]. This behavior can similarly be realized by SM transmit data matrices. Although it is likely that one or more transmit antennas remain inactive in one data block, in general, all channel coefficients would be updated for a sufficiently long transmission period since the selected transmit antenna index is a uniformly distributed random variable.

However, the problem of error propagation resides in all decision-directed channel estimation methods. An incorrectly detected symbol of a previous block may affect the channel estimation performance of its following blocks and produce more symbol errors that continue to propagation along the entire transmission. Hence, pilot signals are inserted periodically and the previous result of channel estimation is forgotten, and the forgetting factor α is introduced to compress the error propagation effect.

The initial guess of channel coefficients is derived by transmitting a full block of pilot signals and estimating with either LS- or MMSE- based methods. These coefficients can

then be updated with decision-directed channel estimation for SM. When MF-based detector is employed, as explained in Chapter 2, we first normalize the column vectors of the estimated channel matrix of the previous ($(k-1)$-th) block time, i.e.,

$$\bar{\mathbf{H}}(k-1) \stackrel{\text{def}}{=} \left[\frac{\hat{\mathbf{h}}_1(k-1)}{\|\hat{\mathbf{h}}_1(k-1)\|}, \cdots, \frac{\hat{\mathbf{h}}_{N_T}(k-1)}{\|\hat{\mathbf{h}}_{N_T}(k-1)\|} \right]. \tag{3.4}$$

Then the received signal of current instant (kth block time) is multiplied by the normalized channel matrix $\bar{\mathbf{H}}(k-1)$ and we have

$$\mathbf{g}_i(k) \stackrel{\text{def}}{=} \begin{bmatrix} g_{1,i}(k) \\ \vdots \\ g_{N_T,i}(k) \end{bmatrix} = \bar{\mathbf{H}}^H(k-1)\mathbf{y}_i(k), \ i = 1, \cdots, B. \tag{3.5}$$

The active transmit antenna index of ith instant of block k can be estimated by finding the maximum value of the MF output:

$$\hat{\ell}_i(k) = \underset{\ell_i \in \{1,\cdots,N_T\}}{\arg\max} |g_{\ell_i,i}(k)|, \tag{3.6}$$

and the carried data is detected via $g_{\ell_i,i}(k)$,

$$\hat{x}_{\hat{\ell}_i}(k) = Q\left(\frac{g_{\hat{\ell}_i}(k)}{\|\hat{\mathbf{h}}_{\hat{\ell}_i}(k-1)\|} \right). \tag{3.7}$$

On the other hand, when ML detector is used, transmit antenna index and data are jointly estimated by

$$(\hat{x}_{\hat{\ell}_i}(k), \hat{\ell}_i(k)) = \arg \min_{(x_i,\ell_i)} \|\mathbf{y}_i(k) - \hat{\mathbf{h}}_{\ell_i}(k-1)x_i\|^2. \tag{3.8}$$

Let $\hat{\mathbf{x}}_i(k) = [0, \cdots, 0, \hat{x}_{\hat{\ell}_i}(k), 0, \cdots, 0]^T$, the estimated data matrix $\hat{\mathbf{X}}(k)$ can be denoted as

$$\hat{\mathbf{X}}(k) = [\hat{\mathbf{x}}_1(k)\ \hat{\mathbf{x}}_2(k), \cdots, \hat{\mathbf{x}}_B(k)], \tag{3.9}$$

which may not be full rank. Define $\mathbb{L} = \{1, \cdots, N_T\}$ as the set of transmit antenna indices and $\hat{\ell}(k) = \{\hat{\ell}_1(k), \cdots, \hat{\ell}_B(k)\}$ the set of active antenna estimates in block k. We flatten $\hat{\mathbf{X}}(k)$ by removing its all-zero rows, which have indices belong to $\mathbb{L} \setminus \hat{\ell}(k)$, and denote the result by $\bar{\mathbf{X}}(k)$.

The channel estimates for the columns indexed by $\hat{\ell}(k)$ are thus

$$\hat{\mathbf{H}}[1,\cdots,N_R;\hat{\ell}(k)](k) \stackrel{def}{=} \mathbf{Y}(k)\bar{\mathbf{X}}^H(k)(\bar{\mathbf{X}}(k)\bar{\mathbf{X}}^H(k))^{-1}. \tag{3.10}$$

While columns that are not updated in this block are kept unchanged and remains the same as the previous block, i.e.,

$$\hat{\mathbf{H}}[1,\cdots,N_R;\mathbb{L}\setminus\hat{\ell}(k)](k) = \hat{\mathbf{H}}[1,\cdots,N_R;\mathbb{L}\setminus\hat{\ell}(k)](k-1). \tag{3.11}$$

However, to ameliorate error propagation effect, we would like to update channel estimate not so abruptly. We define, instead,

$$\hat{\mathbf{H}}(k) = (1-\alpha)\hat{\mathbf{H}}(k) + \alpha\hat{\mathbf{H}}(k-1), \tag{3.12}$$

where $\hat{\mathbf{H}}(k)$ is of the form as (3.10) and (3.12) and $0 \leq \alpha \leq 1$.

We conclude this section by noting that the error-rate performance curve of this scheme has an error floor in high SNR region due to the possibility that not all channel coefficients are updated in each block. Therefore, superimposed pilot signals, which ensure every coefficient is updated, are introduced in next section to improve channel estimation performance.

3.3 SM Channel Estimation With Superimposed Pilots

Superimposed pilot-assisted approaches add (superimposed) low power pilot signal onto the data signals before transmission. At the receiver, the channel can be estimated by these superimposed pilot signals. Unlike the traditional pilot-assisted methods, which do not send any information during the estimation phase, superimposed pilot signals do not cause any loss in transmit data rate. However, this is at the cost of decreasing effective SNR due to the additional power for pilots. In the thesis, we propose a channel estimation method, which combines the decision-directed channel estimation method and use of superimposed pilot signals, for SM schemes.

Note that the initial channel coefficient estimates are acquired by LS or MMSE estimation while after that the estimated coefficients are updated by the detected SM data matrices and imposed pilot signals. Since for an SM system only one transmit antenna is active at a time, other transmit antennas can transmit pilot signals simultaneously to improve the channel estimation quality. The power of superimposed pilots shall be carefully designed because of the following reasons: i) pilots with large powers may cause serious ICI in SM system; and ii) low power pilots do not give reliable estimates.

At the transmitter, data matrix $\mathbf{X}(k)$ and $N_T \times B$ superimposed pilot matrix $\mathbf{S}(k)$ are transmitted at the same time. The received signal is denoted as

$$\mathbf{Y}(k) = \mathbf{H}(k)(\mathbf{X}(k) + \mathbf{S}(k)) + \mathbf{Z}(k), \tag{3.13}$$

Due to the fact that the antenna selection is random, chances are one or more antennas are not active in a block duration. Thus, the transmit data matrix $\mathbf{X}(k)$ might not be full rank and inversible, making channel tracking fails. Nevertheless, this problem may be solved by designing the superimposed pilot matrix $\mathbf{S}(k)$ to be data-dependent. Specifically, the pilot signals are transmitted by transmit antennas which are not used in $\mathbf{X}(k)$ and its corresponding matrix $\mathbf{S}(k)$ has column vectors that span Ker$\{\mathbf{X}(k)\}$ (nullspace of $\mathbf{X}(k)$).

Let $\mathbf{N_x}(k)$ be the matrix consists of a set of basis vector of Ker$\{\mathbf{X}(k)\}$, where it satisfies

$$\mathbf{X}(k)\mathbf{N_x}(k) = \mathbf{0}, \tag{3.14}$$

and the size of $\mathbf{N_x}(k)$ is $B \times M$ with$M$ =Nullity($\mathbf{X}(k)$).

Therefore,

$$\begin{aligned} \mathbf{Y}(k)\mathbf{N_x}(k) &= \mathbf{H}(k)(\mathbf{X}(k) + \mathbf{S}(k))\mathbf{N_x}(k) + \mathbf{Z}(k)\mathbf{N_x}(k) \\ &= \mathbf{H}(k)\mathbf{S}(k)\mathbf{N_x}(k) + \mathbf{Z}(k)\mathbf{N_x}(k). \end{aligned} \tag{3.15}$$

In the following, we detail the design of the superimposed pilot signal matrix for SM systems. For block k, $\mathbf{S}(k)$ has (B-M) nonzero vector, $\mathbf{0}$, and M single-component

columns that have only one nonzero elements on the rows not used by $\mathbf{X}(k)$, where the positions of the nonzero vectors depend on the time instants in which transmit antennas are reused. For example, let both the number of transmit antennas and block size be 4. For a single transmit data matrix

$$\mathbf{X}(k) = \begin{bmatrix} 0 & 0 & 0 & 0 \\ 0 & 0 & 0 & 0 \\ 0 & x_2 & x_3 & x_4 \\ x_1 & 0 & 0 & 0 \end{bmatrix} \text{ or } \mathbf{X}(k) = \begin{bmatrix} x_1 & 0 & 0 & x_4 \\ 0 & 0 & 0 & 0 \\ 0 & x_2 & x_3 & 0 \\ 0 & 0 & 0 & 0 \end{bmatrix}, \tag{3.16}$$

the corresponding superimposed pilot signal matrix can be

$$\mathbf{S}(k) = \begin{bmatrix} 0 & 0 & S_1 & 0 \\ 0 & 0 & 0 & S_2 \\ 0 & 0 & 0 & 0 \\ 0 & 0 & 0 & 0 \end{bmatrix} \text{ or } \mathbf{S}(k) = \begin{bmatrix} 0 & 0 & 0 & 0 \\ 0 & S_2 & 0 & 0 \\ 0 & 0 & 0 & 0 \\ 0 & 0 & 0 & S_4 \end{bmatrix}, \tag{3.17}$$

where S_i's are the superimposed pilot signals with energy E_s.

Due to the SM characteristic (3.15) and the structure of superimposed pilots (3.17), we proposed a channel estimation scheme for this system. It can be summarized by the following procedure:

Step 1: With the detected data matrix $\hat{\mathbf{X}}(k)$, derived by either MF-based or ML detector, we obtain the matrix $\mathbf{N}_{\hat{\mathbf{x}}}(k)$ corresponding to its null space by solving M underdetermined systems of linear equations

$$\bar{\mathbf{X}}(k) \cdot \mathbf{N}_{\hat{\mathbf{x}}}[1, \cdots, B;\ m](k) = \mathbf{0} \tag{3.18}$$

for $m = 1, \cdots, M$, where $\bar{\mathbf{X}}(k) \overset{\text{def}}{=} \hat{\mathbf{X}}[\hat{\ell}(k);\ 1, \cdots, B](k)$.

To simplify channel estimation (in the next step) and incorporate the sparse nature of transmit data matrix, we arrange $\mathbf{N}_{\hat{\mathbf{x}}}(k)$ into a special form such that

$$\bar{\mathbf{S}}[\mathbb{L} \setminus \hat{\ell}(k); 1, \cdots, M](k) = E_s \mathbf{I}_M, \tag{3.19}$$

where $\bar{\mathbf{S}}(k) = \mathbf{S}(k)\mathbf{N}_{\hat{\mathbf{x}}}(k)$. The technique to achieve it is given in Appendix A.

Step 2: With $\mathbf{N}_{\hat{\mathbf{x}}}(k)$ superimposed pilots can be taken out as

$$\bar{\mathbf{Y}}(k) \overset{\text{def}}{=} \mathbf{Y}(k)\mathbf{N}_{\mathbf{x}}(k) = \mathbf{H}(k)\mathbf{S}(k)\mathbf{N}_{\mathbf{x}}(k) + \mathbf{Z}(k)\mathbf{N}_{\mathbf{x}}(k). \tag{3.20}$$

Hence the LS channel estimations on the pilot positions can be obtained as

$$\hat{\mathbf{H}}[1,\cdots,N_R;\mathbb{L}\setminus\hat{\ell}(k)](k)=\bar{\mathbf{Y}}(k)\bar{\mathbf{P}}(k))^H(\bar{\mathbf{P}}(k)\bar{\mathbf{P}}(k))^H)^{-1}. \tag{3.21}$$

Let $\bar{\mathbf{H}}[1,\cdots,N_R;\mathbb{L}\setminus\hat{\ell}(k)](k)\stackrel{\text{def}}{=}\hat{\mathbf{H}}[1,\cdots,N_R;\mathbb{L}\setminus\hat{\ell}(k)](k)$ and $\bar{\mathbf{H}}[1,\cdots,N_R;\hat{\ell}(k)](k)\stackrel{\text{def}}{=}\mathbf{0}$,

$$\bar{\mathbf{Y}}(k)\stackrel{\text{def}}{=}\mathbf{Y}(k)-\bar{\mathbf{H}}(k)\mathbf{S}(k). \tag{3.22}$$

The LS channel estimates for the remaining columns $\hat{\ell}(k)$ are

$$\hat{\mathbf{H}}[1,\cdots,N_R;\hat{\ell}(k)](k)=\bar{\mathbf{Y}}(k)\bar{\mathbf{X}}^H(k)(\bar{\mathbf{X}}(k)\bar{\mathbf{X}}^H(k))^{-1}, \tag{3.23}$$

where $\bar{\mathbf{X}}$ is defined similarly in Section 3.2.

3.4 Simulation Results

In this section, the simulation results of the proposed two channel estimation methods are presented. For a 4×4 MIMO system, we generate each independent path of the spatial uncorrelated time-varying channels by jake's model [35]. The carrier frequency is 2GHz and sampling time T_s is 0.1ms of the duration 10s channel paths. Then the time correlation function is defined as

$$\mathbb{E}\{h_{ij}(t_1)h_{ij}^*(t_2)\}=J_0(2\pi f_D(t_1-t_2)T_s). \tag{3.24}$$

Setting the block length to 4 for the reason that at least 4 symbol times are needed to fully estimate the total number of channel coefficients. The frame size is 5 where the first block consist of pilot signals only. In addition, QPSK constellation is used.

In Figure 3.2 and Figure 3.3, we generate the time-varying channel at mobile velocity 30 km per hour, and compare the bit error rate(BER) and normalized minimum mean square error(NMSE) of decision-directed channel method based on MF-based and ML detector and perfect CSI under the same pilot overhead. It is shown that the performance of decision-directed channel estimation is better than that of only initial pilot estimation is used. Moreover, the decision-directed channel estimation based on ML detector

outperforms MF-based detector. The BER and NMSE performance of decision-directed channel estimation method via different mobile velocity based on MF-based and ML detector are given in Figure 3.4, Figure 3.5, Figure 3.6, and Figure 3.7. It can be seen that there is error floor in high SNR region.

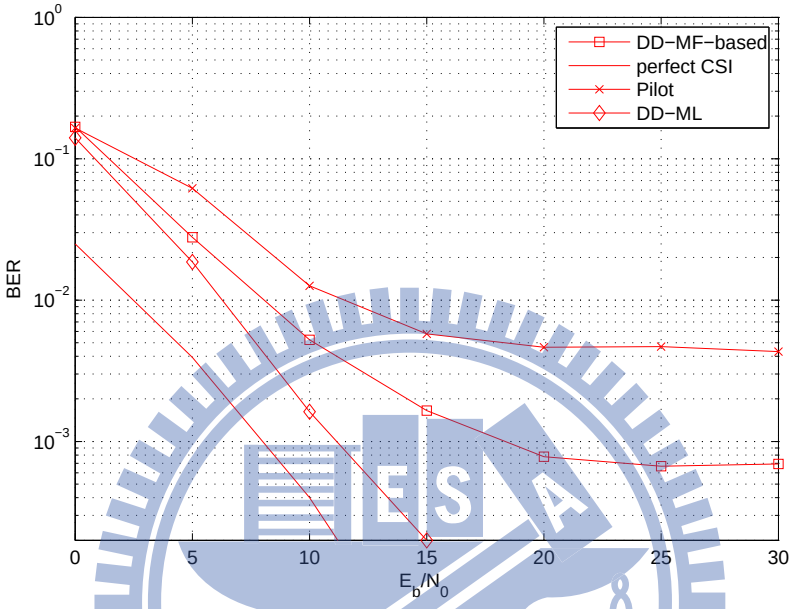

Figure 3.2: BER performance of SM detectors with decision-directed channel estimation.

Superimposed channel estimation method is proposed to improve the error floor performance of decision-directed channel estimation, the energy of superimposed pilot signals affects the BER performance which is shown in Figure 3.8 where the MF-based detector is used and the mobile velocity is set to 30 km/hr. If the energy of superimposed signals is too large, it would cause the serious ICI to receiver and thus degrades the BER performance. However, if the energy is small, it could not have good channel estimation performance. Hence, the optimal energy of the superimposed signal is approximately $2/SNR$ which is shown in Figure 3.9. The BER performance of superimposed channel estimation method under different mobile velocity based on MF-based and ML detector are shown in 3.10 and 3.11, respectively. In addition, we can see from these simulation results that the use of superimposed signal can get better performance than that of

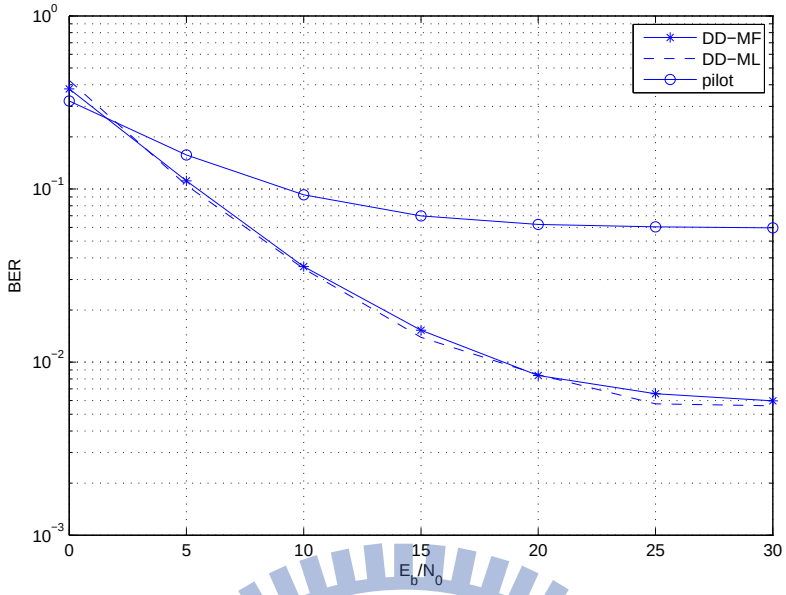

Figure 3.3: NMSE performance of SM detectors with decision-directed channel estimation.

decision-directed channel estimation method in high SNR region and in high mobile velocity.

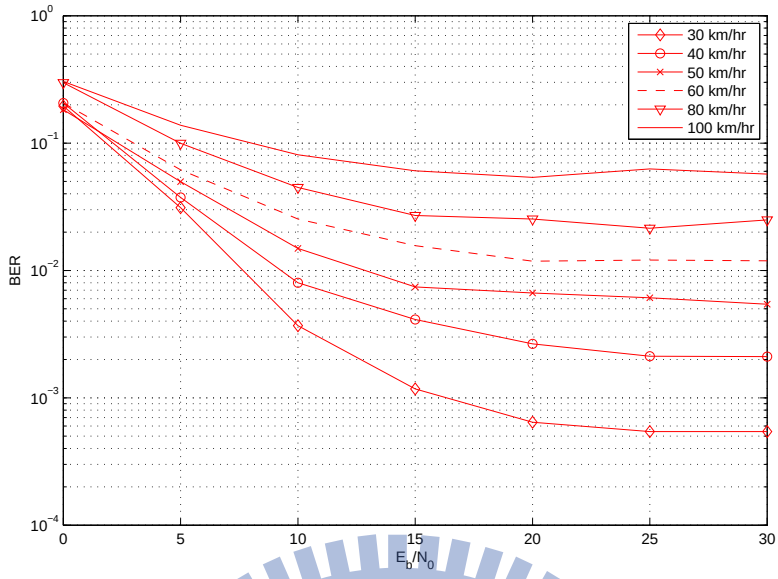

Figure 3.4: BER performance of MF-based detector with decision-directed channel estimation under various mobility.

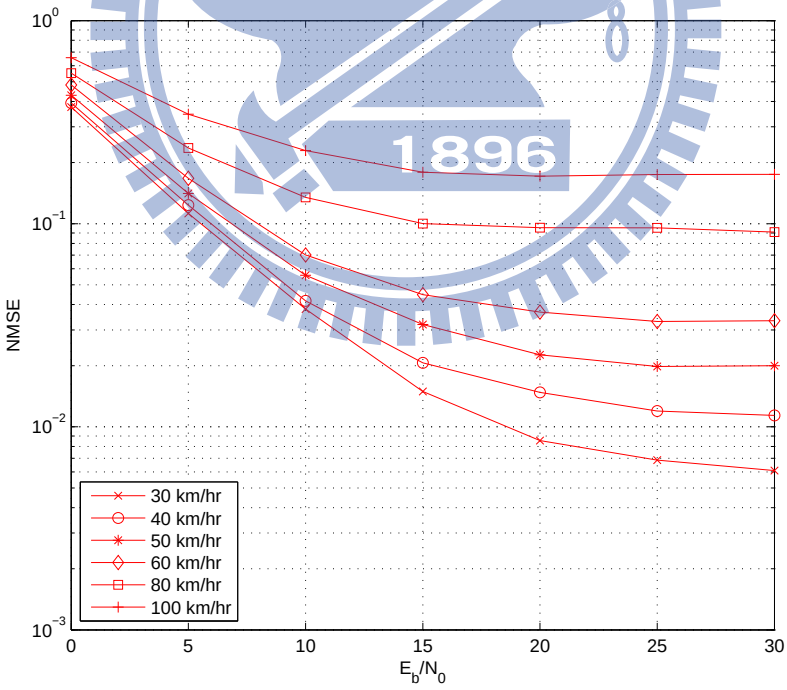

Figure 3.5: NMSE performance of MF-based detector with decision-directed channel estimation under various mobility.

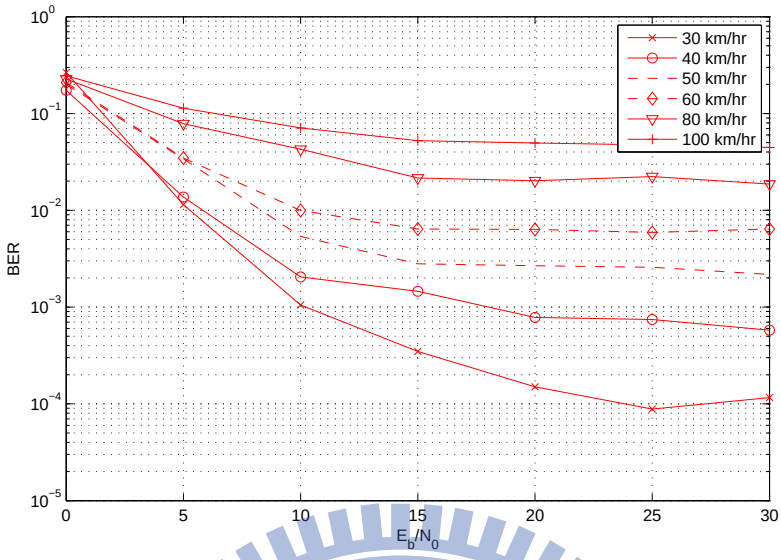

Figure 3.6: BER performance of ML detector with decision-directed channel estimation under various mobility.

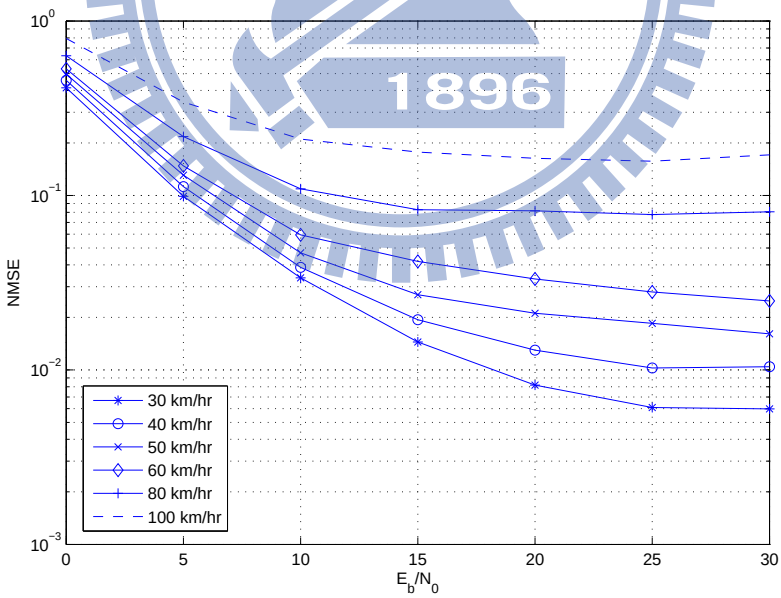

Figure 3.7: NMSE performance of ML detector with decision-directed channel estimation under various mobility.

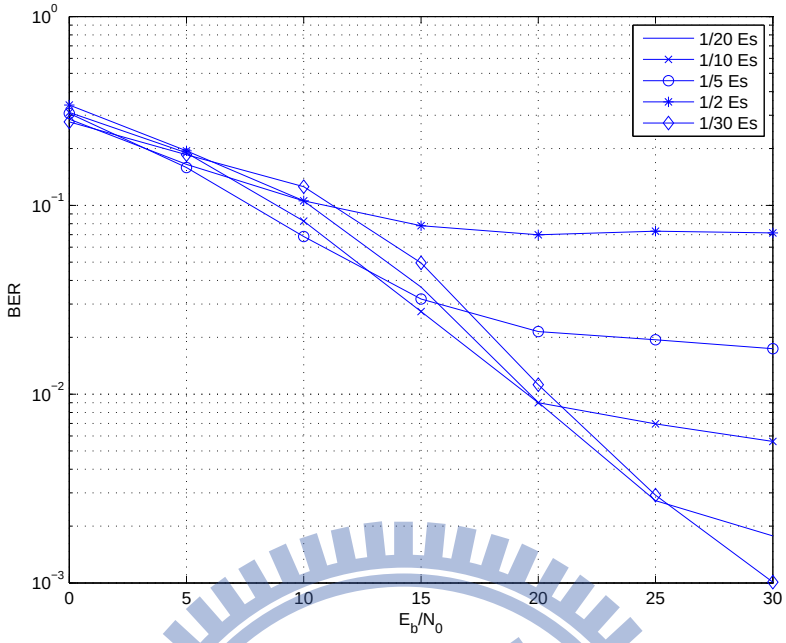

Figure 3.8: BER performance of superimposed channel estimation with different superimposed pilot symbol energy.

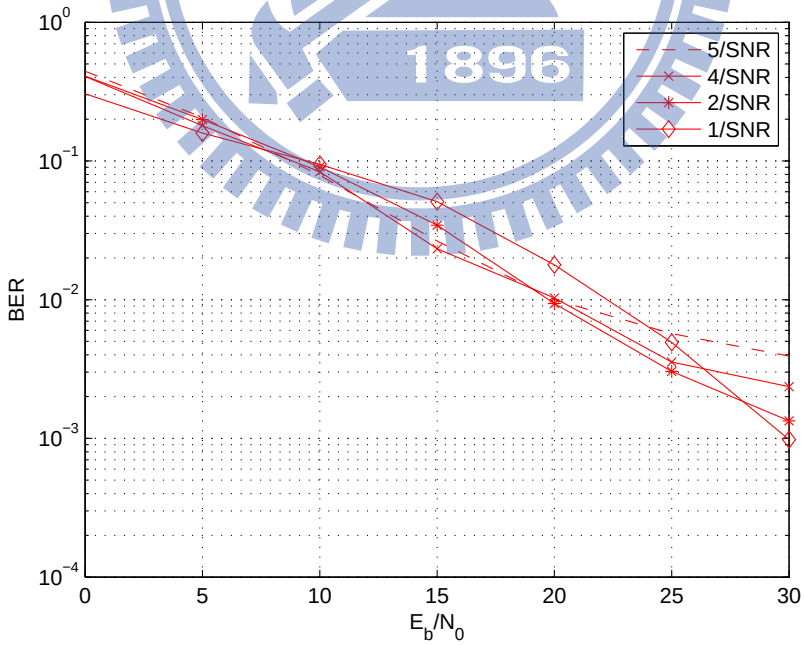

Figure 3.9: BER performance of different superimposed pilot symbol energy versus SNR.

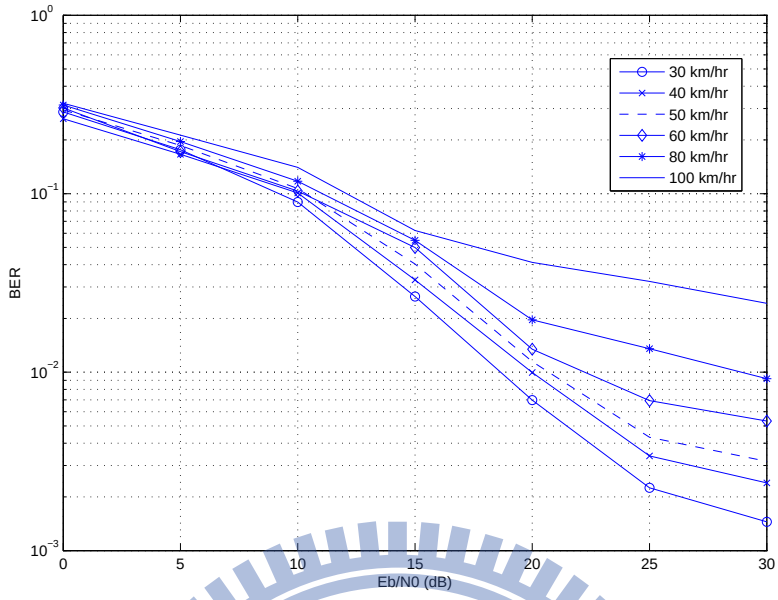

Figure 3.10: BER performance of superimposed channel estimation method with MF-based detector under different mobile velocity.

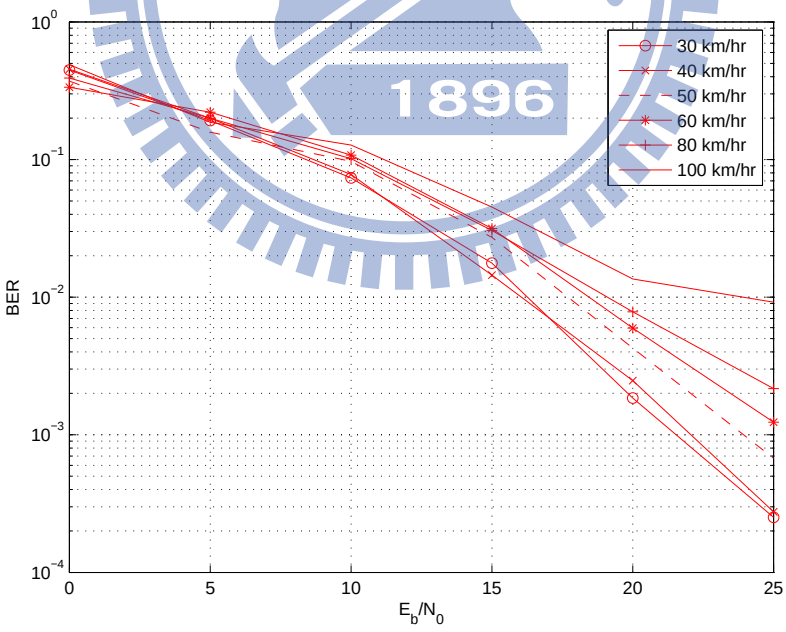

Figure 3.11: BER performance of superimposed channel estimation method with ML detector under different mobile velocity.

Chapter 4

Spatial Modulation Using Dual-Polarized Antenna Arrays

4.1 Dual-Polarized MIMO Channel Models

In MIMO wireless communication systems, antenna spacings are usually required to be at least half a wavelength at subscriber units and ten wavelengths at base stations to achieve satisfactory performance. This condition restricts the implementation of MIMO systems on some space-limited devices. However, since orthogonal polarization can decrease the correlation of transmit antennas or receive antennas, the usage of co-located dual-polarized antennas can be a space- and cost-effective alternative. Figure 4.1 depicts a co-located dual-polarized MIMO system with antennas grouped into pairs.

For ideal dual-polarized antennas, cross-polar transmissions, from a vertically-polarized transmit antenna to a horizontally-polarized receive antenna or from a horizontally-polarized transmit antenna to a vertically-polarized receive antenna, equal to zero. Practically, there are two depolarization mechanisms that can cause polarization interference: cross-polar isolation (XPI) due to use of imperfect antennas and the depolarization caused by the propagation channel which can be identified by the existence of cross-polar ratio (XPR). The interplay between both effects forms the global cross-polar discrimination (XPD) which quantifies the separation between two channels of different

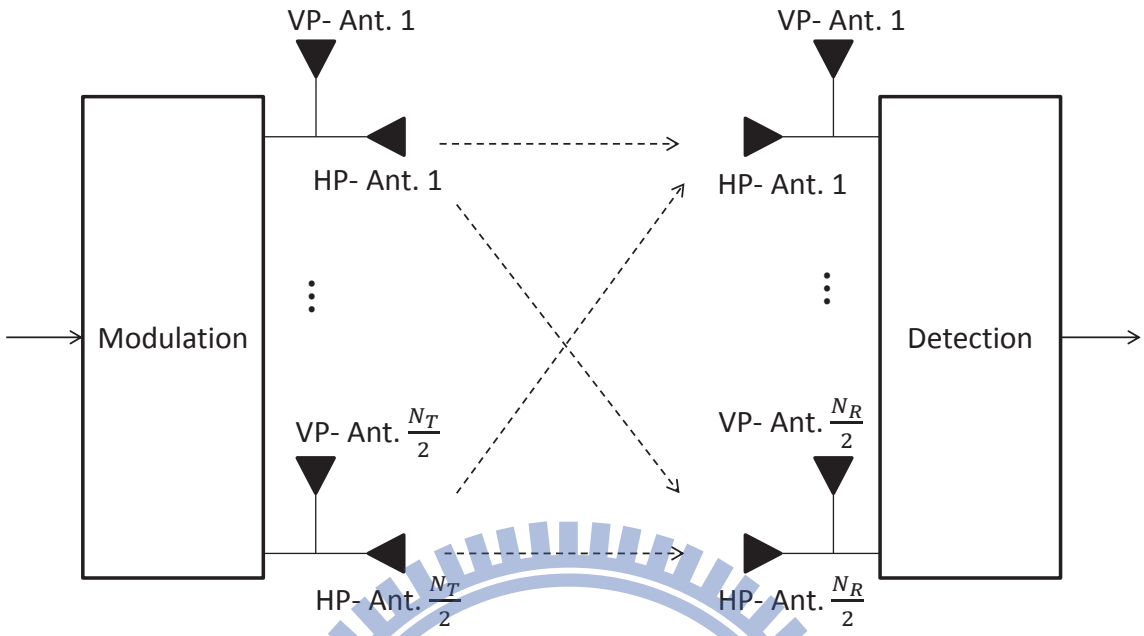

Figure 4.1: A co-located dual-polarized MIMO system model.

polarizations. Besides, vertically-polarized electromagnetic wave is vulnerable to electric current on the ground, so co-polar ratio (CPR) can be taken into consideration in some cases. Figure 4.2 shows the depolarization mechanisms discussed above.

We first consider one dual-polarized transmit-receive antenna pair, Let $p_{ij} \stackrel{\text{def}}{=} |h_{ij}|^2$ $(i, j \in \{V, H\})$ be the instantaneous dual-polarized channel gain. The channel is a 2×2 matrix,

$$\mathbf{H}_P = \begin{bmatrix} h_{VV} & h_{VH} \\ h_{HV} & h_{HH} \end{bmatrix}, \tag{4.1}$$

and depolarization parameters can be defined as

(1) Cross-polar isolation:

$$\text{Transmitter} : \mathbf{XPI}_T \stackrel{\text{def}}{=} \frac{\mathbb{E}\{p_{ii}\}}{\mathbb{E}\{p_{ij}\}} \tag{4.2}$$

$$\text{Receiver} : \mathbf{XPI}_R \stackrel{\text{def}}{=} \frac{\mathbb{E}\{p_{ii}\}}{\mathbb{E}\{p_{ji}\}} \tag{4.3}$$

(2) Cross-polar ratio:

$$\mathbf{XPR} \stackrel{\text{def}}{=} \frac{p_{vv}}{p_{hv}} = \frac{p_{hh}}{p_{vh}} \tag{4.4}$$

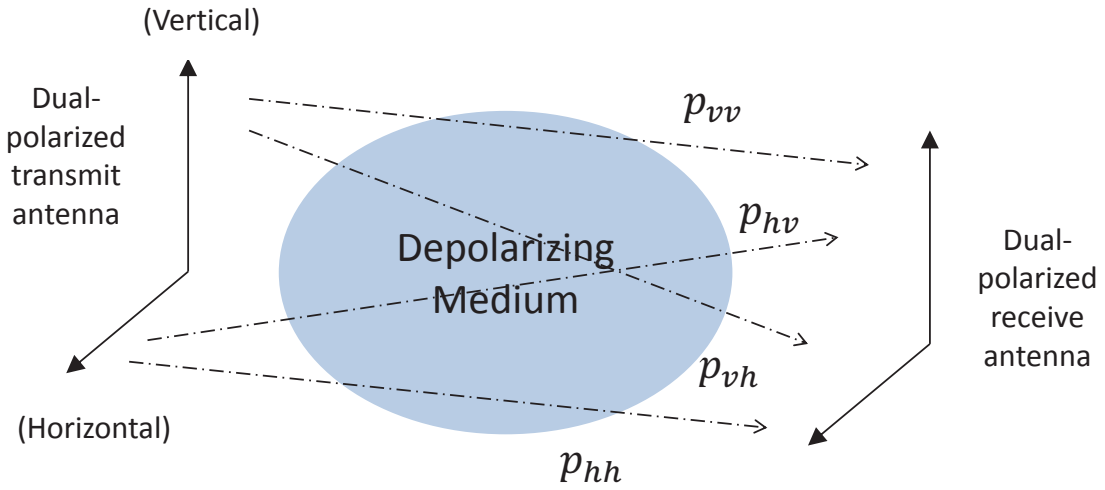

Figure 4.2: Depolarization mechanisms.

(3) Co-polar ratio:

$$\mathbf{CPR} \stackrel{\text{def}}{=} \frac{p_{vv}}{p_{hh}} \tag{4.5}$$

Analytically, XPI effect at transmitter and receiver can be respectively modelled with coupling matrices

$$\mathbf{M}_t = \begin{bmatrix} 1 & \sqrt{\chi_{a,t}} \\ \sqrt{\chi_{a,t}} & 1 \end{bmatrix}, \tag{4.6}$$

$$\mathbf{M}_r = \begin{bmatrix} 1 & \sqrt{\chi_{a,r}} \\ \sqrt{\chi_{a,r}} & 1 \end{bmatrix}, \tag{4.7}$$

where $\chi_{a,t}$ and $\chi_{a,r}$ are the inverse of XPI at transmitter and receiver, respectively. If the used dual-polarized antennas are in perfect condition, these scalars will equal to zeros. Note that this depolarization mechanism affect line-of-sight (LOS) and scattered components whereas XPR exists only in non-line-of-sight components.

While the above definitions concentrate only on the channel gains, to get a thorough understanding of the depolarization effect, the dual-polarized channel can be characterize by the correlation matrix $\mathbb{E}\{vec(\mathbf{H}_P^H)vec(\mathbf{H}_P^H)^H\}$. The diagonal terms of this 4×4 matrix are the average channel gains of each channel coefficient and the off-diagonal ones include the cross-polar correlations (XPC) between h_{ii} and h_{ij} or h_{ji}, co-polar correlation (CPC)

between h_{vv} and h_{hh}, and anti-polar correlation (APC) between h_{vh} and h_{hv}. This model is verified by several measurements to be a good approximation to the real dual-polarized channels. The corresponding parameters to various environment settings are given in [19] and references therein.

In the following, one dual-polarized antenna pair is extended to a MIMO system. As the measurement result [19] shown, in Rayleigh fading environment, the spatial correlation properties are independent of the polarization, i.e., beam pattern are similar for all antennas, the parameters concerning the polarization and spatial correlation can be decoupled in our model. It is especially true when the system is implemented in macrocells or microcells. It is explained in the following.

An $N_R \times N_T$ dual-polarized MIMO fading channel consists of $N_T/2$ and $N_R/2$ co-located dual-polarized transmit and receive antenna pairs. If all dual-polarized antennas are identically oriented, the joint transmitter-to-receiver direction spectrum would be equivalent for all co-located antennas. The matrix can thus be written as

$$\tilde{\mathbf{H}}_{\mathrm{x}} = \mathbf{H}_{\frac{N_R}{2}\times\frac{N_T}{2}} \otimes \mathbf{M}_r \tilde{\mathbf{W}} \mathbf{M}_t \tag{4.8}$$

where $\mathbf{H}_{N_R/2\times N_T/2}$ is the spatial correlated Rayleigh fading channel and $\tilde{\mathbf{W}}$ is the de-polarization matrix which is separated from the spatial correlation parameters. Matrix $\tilde{\mathbf{W}}$ models the differential attenuation and the correlated phase shifts between the dual-polarized channels. Specifically,

$$vec(\tilde{\mathbf{W}}^H) = \begin{bmatrix} 1 & \sqrt{\mu\chi}\vartheta^* & \sqrt{\chi}\sigma^* & \sqrt{\mu}\delta_1^* \\ \sqrt{\mu\chi}\vartheta & \mu\chi & \sqrt{\mu\chi}\delta_2^* & \mu\sqrt{\chi}\sigma^* \\ \sqrt{\chi}\sigma & \sqrt{\mu\chi}\delta_2 & \chi & \sqrt{\mu\chi}\vartheta^* \\ \sqrt{\mu}\delta_1 & \mu\sqrt{\chi}\sigma & \sqrt{\mu\chi}\vartheta & \mu \end{bmatrix}^{1/2} vec(\tilde{\mathbf{W}}_\omega^H), \tag{4.9}$$

where μ and χ represent the inverse of CPR and XPR, σ and ϑ are the receive and transmit correlation coefficients between polarization vv and hv, hh and hv, vv and vh or hh and vh. δ_1 and δ_2 are respectively co- and anti-polar correlation coefficients. The last term,

$$\tilde{\mathbf{W}}_\omega \stackrel{\text{def}}{=} \begin{bmatrix} e^{j\Phi_1} & e^{j\Phi_2} \\ e^{j\Phi_3} & e^{j\Phi_4} \end{bmatrix}, \tag{4.10}$$

where Φ_k's are uniformly distributed in $[0, 2\pi)$.

As a result, a dual-polarized MIMO channel can be formed into

$$\tilde{\mathbf{H}}_{\mathrm{x}} = \begin{bmatrix} \mathbf{H}_{1,1} & \mathbf{H}_{1,2} & \dots & \mathbf{H}_{1,\frac{N_T}{2}} \\ \mathbf{H}_{2,1} & \mathbf{H}_{2,2} & \dots & \mathbf{H}_{2,\frac{N_T}{2}} \\ \vdots & \vdots & \vdots & \vdots \\ \mathbf{H}_{\frac{N_R}{2},1} & \mathbf{H}_{\frac{N_R}{2},2} & \dots & \mathbf{H}_{\frac{N_T}{2},\frac{N_T}{2}} \end{bmatrix}, \tag{4.11}$$

where $\mathbf{H}_{i,j}$ is the dual-polarized channel matrix of the jth transmit and ith receive antenna pairs:

$$\mathbf{H}_{i,j} = \begin{bmatrix} h_{iVjV} & h_{iVjH} \\ h_{iHjV} & h_{iHjH} \end{bmatrix}. \tag{4.12}$$

where each entry $h_{iP_ijP_j}$ is the channel coefficient between the P_i-polarized ith transmit antenna pair and P_j-polarized $j$the receive antenna pair. In addition, we define the column vectors of $\tilde{\mathbf{H}}_{\mathrm{x}}$ as

$$\tilde{\mathbf{H}}_{\mathrm{x}} = \left[\mathbf{h}_{1V}, \mathbf{h}_{1H}, \cdots \mathbf{h}_{\frac{N_T}{2}V}, \mathbf{h}_{\frac{N_T}{2}H}\right]. \tag{4.13}$$

4.2 Dual-Polarized Spatial-Correlated (DPSC) Channel Model

Most of the previous proposals model spatial correlated channels by the Kronecker model which is not reasonable when joint correlation exists between transmitter and receiver. A more general model [27] has been discussed in Chapter 2 and is considered here to incorporate with the dual-polarized systems.

We assume the XPIs of all dual-polarized antenna pairs are infinite, i.e., the transmit and receive antenna in a pair are perfectly polarized. Matrices $\mathbf{M}_r$ and $\mathbf{M}_t$ become identity and are thus ignored in the following discussion. A dual-polarized MIMO channel is denoted as

$$\tilde{\mathbf{H}}_{\mathrm{x}} = \mathbf{H}_{\frac{N_R}{2}\times\frac{N_T}{2}} \otimes \tilde{\mathbf{W}}. \tag{4.14}$$

It has been proven that 4.14 can be equally represented by

$$\tilde{\mathbf{H}}_{\mathrm{x}} = \mathbf{Q}_{N_R,K_R}\tilde{\mathbf{C}}\mathbf{Q}^H_{N_T,K_T}, \tag{4.15}$$

where $\tilde{\mathbf{C}}$ is complex random and $\mathbf{Q}_{N_R,K_R}$ and $\mathbf{Q}_{N_T,K_T}$ are $N_R \times K_R$ and $N_T \times K_T$ predefined unitary matrices, respectively with K_R ($\leq N_R$) and K_T ($\leq N_T$) being the modelling orders to be discussed later [27].

Several types of functions can be chosen as (basis) vectors in the predefined unitary matrices [27]. In this thesis, polynomial basis functions [32] are used. Specifically, these polynomial functions are of degree D where the entries of the corresponding basis matrix $\mathbf{D}$ are specified as

$$[\mathbf{D}]_{i,j} = (i-1)^{j-1}, \ i,j = 1,2,\cdots,D, \tag{4.16}$$

where D equals to N_T when $\mathbf{D}$ is used to determine $\mathbf{Q}_{N_T,K_T}$ and N_R to determine $\mathbf{Q}_{N_R,K_R}$. Consider first the construction of $\mathbf{Q}_{N_T,K_T}$. In order to satisfy the unitary property, by applying QR decomposition, we can obtain the orthonormal polynomial basis matrix $\mathbf{Q}$, i.e., $\mathbf{D} = \mathbf{QR}$. Then, we can choose the first K_T columns of $\mathbf{Q}$ to be the predefined matrices $\mathbf{Q}_{N_T,K_T}$ where modelling order K_T can be determined by Akaike information criterion (AIC) or minimum description length (MDL) approach [33]. $\mathbf{Q}_{N_R,K_R}$ is obtained analogously.

Due to the property that co-located dual-polarized antennas experience the same spatial characteristics, we are able to reduce the degree of this basis matrix D to half of the original DPSC MIMO channel model is thus modified to

$$\tilde{\mathbf{H}}_{\mathrm{x}} = (\mathbf{Q}_{\frac{N_R}{2},K_R} \otimes \mathbf{I}_2)\mathbf{C}(\mathbf{Q}^H_{\frac{N_T}{2},K_T} \otimes \mathbf{I}_2), \tag{4.17}$$

$$\mathbf{C} = \tilde{\mathbf{C}} \otimes \tilde{\mathbf{W}}, \tag{4.18}$$

where the depolarization effect is coupled into $\mathbf{C}$ and the modelling orders $K_R \leq \frac{N_R}{2}$ and $K_T \leq \frac{N_T}{2}$. With predefined $\mathbf{Q}_{\frac{N_R}{2},K_R}$ and $\mathbf{Q}_{\frac{N_T}{2},K_T}$, identification of the unknown channel $\tilde{\mathbf{H}}_{\mathrm{x}}$ is equivalent to the estimation of $\tilde{\mathbf{C}}$, which usually has fewer unknowns than those of $\tilde{\mathbf{H}}_{\mathrm{x}}$.

4.3 Time-Varying DPSC Channel Estimation

Let $\mathbf{X}_P(k)$ be $N_T \times B$, a full-rank pilot matrix used to estimate time-varying DPSC channel $\tilde{\mathbf{H}}_{\mathrm{x}}$. The received signal can be expressed as

$$\begin{aligned} \mathbf{Y}_P(k) &= \tilde{\mathbf{H}}_{\mathrm{x}}(k)\mathbf{X}_P(k) + \mathbf{Z}_P(k) \\ &= (\mathbf{Q}_{\frac{N_R}{2},K_R} \otimes \mathbf{I}_2)\tilde{\mathbf{C}}(k)(\mathbf{Q}^H_{\frac{N_T}{2},K_T} \otimes \mathbf{I}_2)\mathbf{X}_P(k) + \mathbf{Z}_P(k). \end{aligned} \tag{4.19}$$

where $\mathbf{Q}_{\frac{N_T}{2},K_T}$, $\mathbf{Q}_{\frac{N_R}{2},K_R}$, and $\mathbf{X}_P(k)$ are known to the receivers. By a property of vector operation, we have

$$vec(\mathbf{ABC}) = (\mathbf{C}^T \otimes \mathbf{A})vec(\mathbf{B}). \tag{4.20}$$

Due to the fact that (4.20),

$$\begin{aligned} vec(\mathbf{Y}_P(k)) &= \left[(\mathbf{X}_P(k)^H(\mathbf{Q}_{N_T/2,K_T} \otimes \mathbf{I}_2)) \otimes (\mathbf{Q}_{N_R/2,K_R} \otimes \mathbf{I}_2)\right] vec(\mathbf{C}(k)) \\ &\quad + vec(\mathbf{Z}_P(k)), \end{aligned} \tag{4.21}$$

the LS estimate of $\mathbf{C}(k)$ can be obtained as

$$vec(\hat{\mathbf{C}}(k)) = (\mathbf{V}^H\mathbf{V})^{-1}\mathbf{V}^H vec(\mathbf{Y}_P(k)), \tag{4.22}$$

where $\mathbf{V} \overset{\text{def}}{=} \left(\mathbf{X}_P(k)^H(\mathbf{Q}_{N_T/2,K_T} \otimes \mathbf{I}_2)\right) \otimes (\mathbf{Q}_{N_R/2,K_R} \otimes \mathbf{I}_2)$.

Note that the decision-directed channel estimation technique proposed in Chapter 3 can also be utilized here by substituting $\mathbf{X}_P(k)$ in (4.22) by $\hat{\mathbf{X}}(k)[\hat{\ell}(k); 1, \cdots, B](k)$. The detection algorithms for SM in dual-polarized channel are discussed in the next subsection.

4.4 Data Detection in SM-DPSC Channels

When co-located dual-polarized in the SM system, information is conveyed by the index of the transmit antenna pair and the specific polarization in that pair used and the symbol transmitted. Hence, $m = \log_2(N_T M)$ bits are transmitted in each channel

use. The receiver's task thus contains the used transmit antenna and polarization index estimation and transmitted symbol detection. The system model is depicted in Figure 4.3. A mapping rule for this SM system with two dual-polarized antenna pairs in both the transmitter and receiver and BPSK or QPSK modulated symbols is suggested in Table 4.1

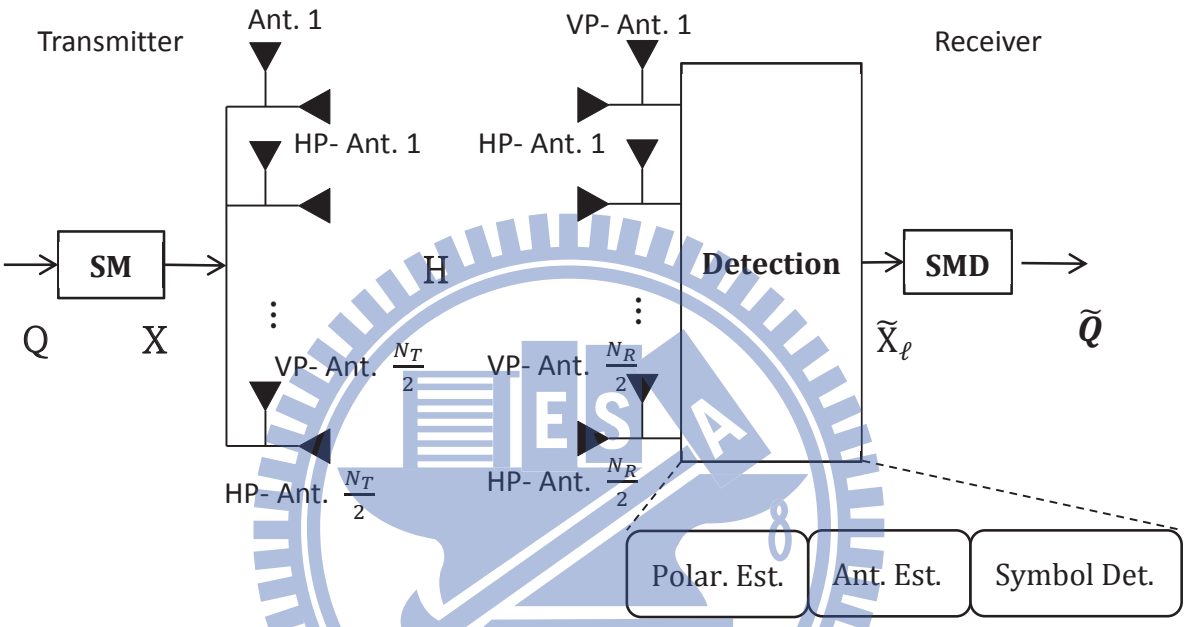

Figure 4.3: A dual-polarized SM system model.

Three data detection techniques are proposed for the spatial modulated dual-polarized MIMO system. Since we only concentrate on its data detection in this section, CSI $\tilde{\mathbf{H}}_{\mathrm{x}}$ is assumed known at the receiver and block index k is ignored. The received signal corresponding to transmitted signal $\mathbf{X}$ can be represented as

$$\mathbf{Y} = \tilde{\mathbf{H}}_{\mathrm{x}}\mathbf{X} + \mathbf{Z}. \tag{4.23}$$

The ML detector is simply

$$(\hat{x}_i, \hat{\ell}_i) = \arg\min_{x_i,\ell_i} \|\mathbf{y}_i - \tilde{\mathbf{h}}_{\mathrm{x},\ell_i} x_i\|^2, \ i = 1, \cdots, B. \tag{4.24}$$

Input bits	Antenna Index	Transmit Symbol		Antenna Index	Transmit Symbol
000	VP-1	+1		VP-1	+1 + j
001	VP-1	-1		VP-1	-1 + j
010	HP-1	+1		VP-1	-1 - j
011	HP-1	-1		VP-1	+1 - j
100	VP-2	+1		HP-1	+1 + j
101	VP-2	-1		HP-1	-1 + j
110	HP-2	+1		HP-1	-1 - j
111	HP-2	-1		HP-1	+1 - j

Table 4.1: An SM mapping table for the dual-polarized system for 3 bits/transmission

The MF-based detector for (4.24) is similar to the traditional one (2.16)-(2.21) for (2.3) with following procedure:

$$\bar{\mathbf{H}} = \left[\frac{\tilde{\mathbf{h}}_{\mathrm{x},1}}{\|\tilde{\mathbf{h}}_{\mathrm{x},1}\|}, \cdots, \frac{\tilde{\mathbf{h}}_{\mathrm{x},N_T}}{\|\tilde{\mathbf{h}}_{\mathrm{x},N_T}\|}\right], \tag{4.25}$$

$$\mathbf{g}_i = \bar{\mathbf{H}}^H \mathbf{y}_i, \tag{4.26}$$

$$\hat{\ell}_i = \underset{\ell_i \in \{1,\cdots,N_T\}}{\arg\max} |g_{\ell_i,i}|, \tag{4.27}$$

$$\hat{x}_{\ell_i} = \mathcal{Q}\left(\frac{g_{\hat{\ell}_i,i}}{\|\tilde{\mathbf{h}}_{\mathrm{x},\hat{\ell}_i}\|}\right),\ i = 1, \cdots, B. \tag{4.28}$$

Prior to the introduction of the last detection method, we consider the following.

Since antenna polarization selection bares information for SM system in dual-polarized MIMO system, we shall give a few facts. Based on the Cauchy-Schwarz inequality, for a specific spatial channel i (the ith column of $\tilde{\mathbf{H}}_{\mathrm{x}}$, $\mathbf{h}_i$), we have the following due to the mismatch of polarization:

$$\frac{|\mathbf{h}_{iV}^H \mathbf{h}_{iH}|}{\|\mathbf{h}_{iH}\|} \le \frac{|\mathbf{h}_{iV}^H \mathbf{h}_{iV}|}{\|\mathbf{h}_{iV}\|} = \|\mathbf{h}_{iV}\| \tag{4.29}$$

which agree with our intuition. On the other hand, for two different spatial channel vectors, say $\mathbf{h}_i$ and $\mathbf{h}_j$, the correlation between their portions corresponding to the same polarization outweighs that corresponding to different polarizations, i.e.,

$$\frac{|\mathbf{h}_{iV}^H \mathbf{h}_{jH}|}{\|\mathbf{h}_{jH}\|} \le \frac{|\mathbf{h}_{iV}^H \mathbf{h}_{jV}|}{\|\mathbf{h}_{jV}\|} \le \|\mathbf{h}_{iV}\|. \tag{4.30}$$

This is because of the inability of a polarized antenna to receive signal of other polarizations. In this way, the (horizontal) polarization of a signal passing through $\mathbf{h}_{iV}$ can be effective estimated prior to the antenna and symbol detection.

As a result, the polarization used can be detected before ML detection of antenna pair index and symbol. This suboptimal method effectively lower the complexity of detection algorithm with some performance loss. Specifically, first calculate (4.24) and find the MF output of vertical or horizontal polarized transmit antenna of each transmit antenna pair,

$$\hat{\mathbf{n}}_P = [\hat{n}_V \ \hat{n}_H] = \sum_{i=1}^{\frac{N_T}{2}} \arg\max_{\mathbf{n}_P \in \{[1,0],[0,1]\}} \left| \bar{\mathbf{h}}_{iV}^H \mathbf{y} \cdot n_{P,1} + \bar{\mathbf{h}}_{iH}^H \mathbf{y} \cdot n_{P,2} \right| \tag{4.31}$$

where $\mathbf{n}_P$ is the indicator vector whose position of value 1 represents the detected polarization in a specific transmit antenna pair and $\hat{n}_V$ and $\hat{n}_H$ count the total number of detected polarization used in all transmit antenna pairs. Based on the majority vote algorithm, the used polarization of the transmit antenna is decided via

$$\hat{P} = \arg\max_{P=V,H} \{\hat{n}_V \ \hat{n}_H\} \tag{4.32}$$

Based on the result, the ML detector of the antenna pair used and symbol transmitted only needs to search over the specific $\hat{P}$-polarized channel vectors,

$$(\hat{x}_i, \hat{\ell}_i) = \arg\min_{x_i, \ell_i = i\hat{P}} \|\mathbf{y}_i(k) - \tilde{\mathbf{h}}_{\mathrm{x},\ell_i} x_i\|^2, \ i = 1, \ldots, B. \tag{4.33}$$

This detection method reserves the high detection performance of the ML detector but needs only about half of the complexity required by the latter. As will be shown later, it outperform the MF-based detector.

4.5 Simulation Results

In this section, we investigate the performance of SM scheme using dual-polarized antenna. For simplicity and the measurement results in [19], we concentrate on the effect

of XPR and CPR. The values of μ and χ are set to 0.7 and 0.1 for all the simulation results except for Figure 4.8 and Figure 4.9, and the parameters of polarized correlation are set to zero. First, the BER performance of 2×2 SM comparing to 4×4 SM using dual-polarized antenna is given in Figure 4.4 where MF-based detector is used and CSI is assumed known to receiver. We can see from the result that the use of dual-polarized antennas can give the polarization diversity gain.

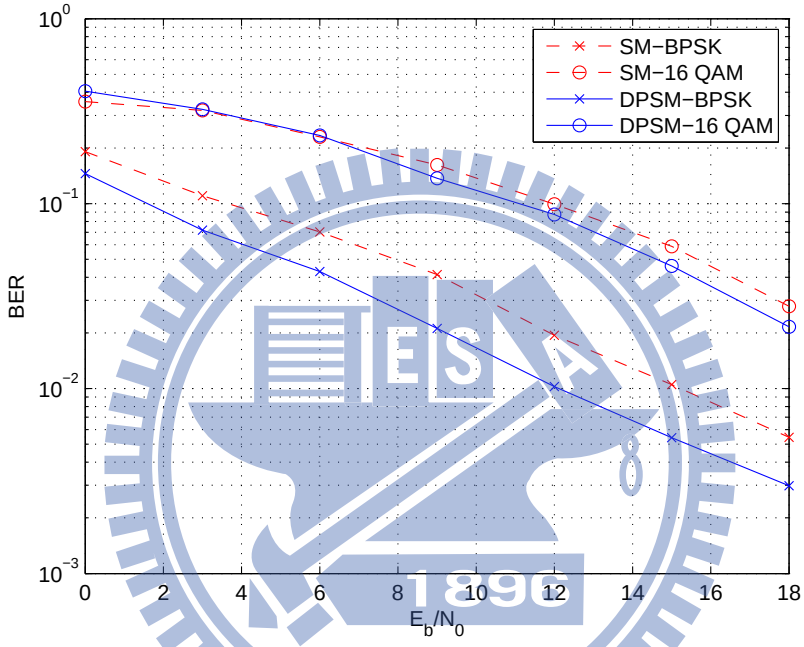

Figure 4.4: Comparison of BER performance for SM under conventional MIMO channel and dual-polarized MIMO channel.

We also give a BER performance comparison between SM and V-BLAST and space time code based on Alamouti[4] under dual-polarized channel in Figure 4.5. Based on the same spectral efficiency which is 8 bits/transmission, SM outperforms V-BLAST and Alamouti scheme. V-BLAST in this simulation result uses QR-based detector and Alamouti and SM scheme use ML detector.

Then the normalized mean square error of dual-polarized spatial correlated channel estimation method is shown in Figure 4.6. In this figure, we use the 3GPP SCM model

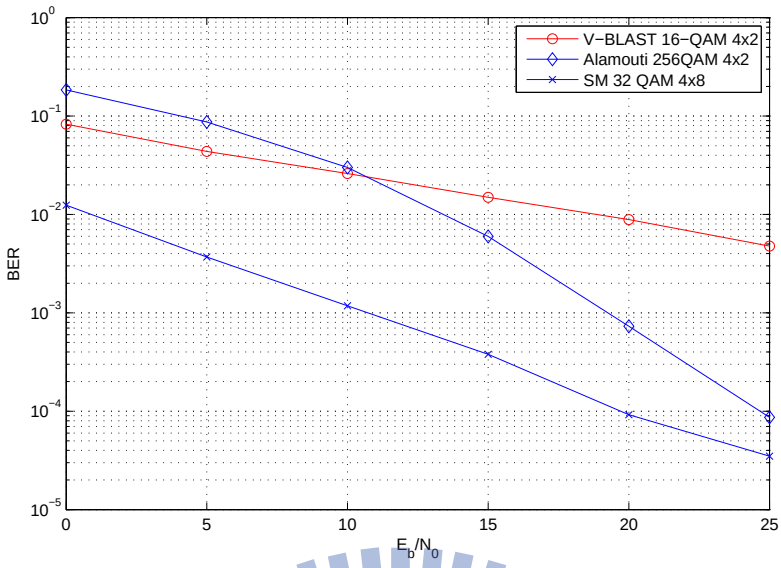

Figure 4.5: Comparison of BER performance for SM and VBLAST and Alamouti scheme under dual-polarized channel for 8 bits/transmission.

to generate the co-located dual-polarized spatial correlated channel. Two channels with different angle spread (AS) 2 and 15 with mobile velocity 60 km/hr are adopted in the simulation result. The number of transmit and receive antennas setting to 8, we compare the NMSE performance of conventional MIMO channel estimation methods and modified dual-polarized channel estimation method. It can be seen from this figure that dual-polarized spatial correlated channel estimation method only use half of the basis to achieve the same estimation performance with conventional method.

The BER performance of proposed detectors for SM in dual-polarized system is shown in Figure 4.7. We consider a 4×4 MIMO channel using dual-polarized antennas, and QPSK modulated signals. From the result, ML detector performs the best of three detectors and the low-complexity sub-optimal detector outperforms MF-based detector where we assume CSI is known to receiver in this simulation result. We also investigate the influence on the three detectors of depolarization effect caused by propagation channel. From Figure 4.8, fixed parameter χ to 0.5, when the value μ is too small, all the three detectors can not have adequate performance because the horizontal-polarized channel

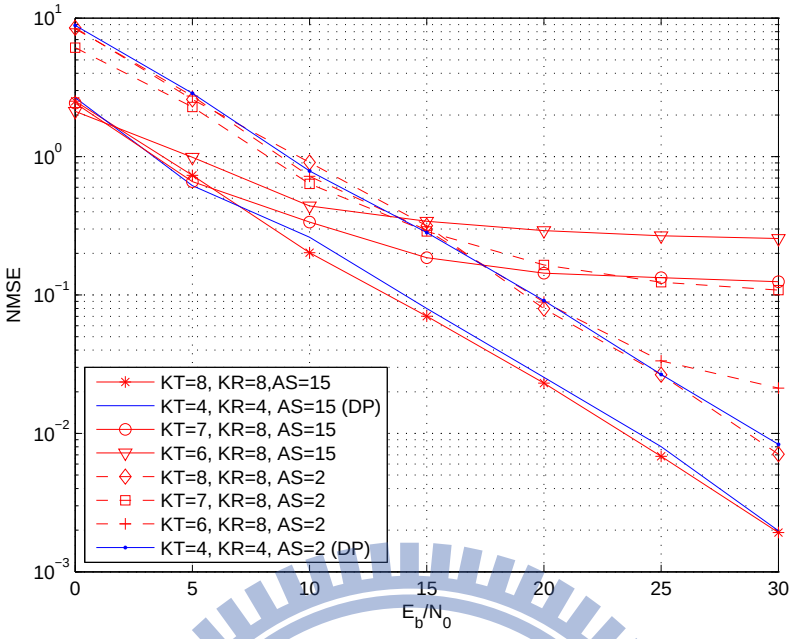

Figure 4.6: NMSE comparison of channel estimation for dual-polarized spatial-correlated MIMO channel with different modelling order, AS=2 and 15.

is too small than vertical and thus cause the signals transmit by horizontal-polarized antenna cannot be successfully detected. The effect of χ which denotes the inverse of XPR value with fixed $\mu = 0.5$ on the detectors's performance is given in Figure 4.9. The result shows that when the value of χ is too large which means that cross interference between polarization is large, the performance of the MF-based and the suboptimal detector degrade since the large χ value can make the channel vector of vertical- and horizontal-polarized transmit antenna become similar thus the value of MF output of both the vertical and horizontal polarized antenna are approximately equal. Therefore, the MF-based and suboptimal detectors cannot detect the polarization correctly.

The following part, we give the simulation result of different time-varying channel estimation methods in DPSC channel where t and r are assumed to be 0.3, and three detectors are investigated. In Figure 4.10–4.15, the BER and NMSE performance of decision-directed channel estimation method based on MF-based, suboptimal and ML

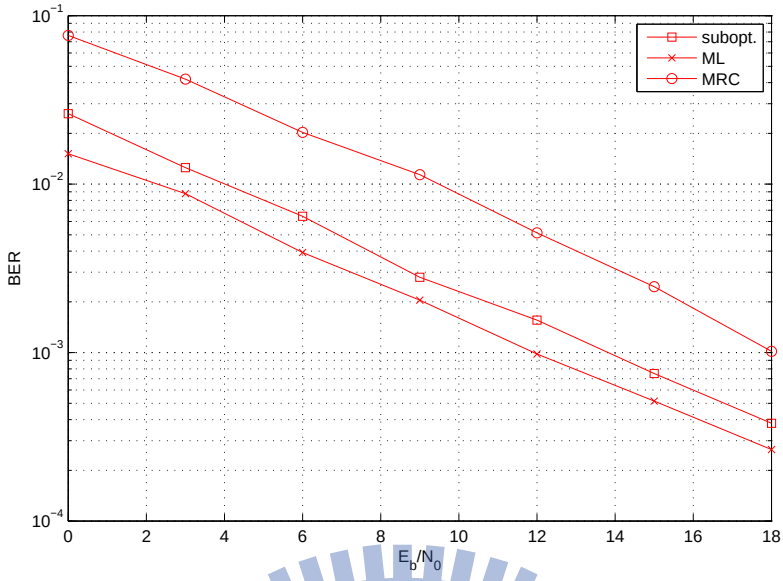

Figure 4.7: Comparison of BER performance of SM for MF-based detector, suboptimal detector and ML detector under perfect CSI.

detector are shown, we can see that using ML or suboptimal detectors can have better performance than that of MF-based detector. In addition, the performance loss increase when the mobile velocity increases. In Figure 4.16, BER performance of superimposed channel estimation method is given. It performs better than decision-directed channel estimation in high SNR and fast varying channel.

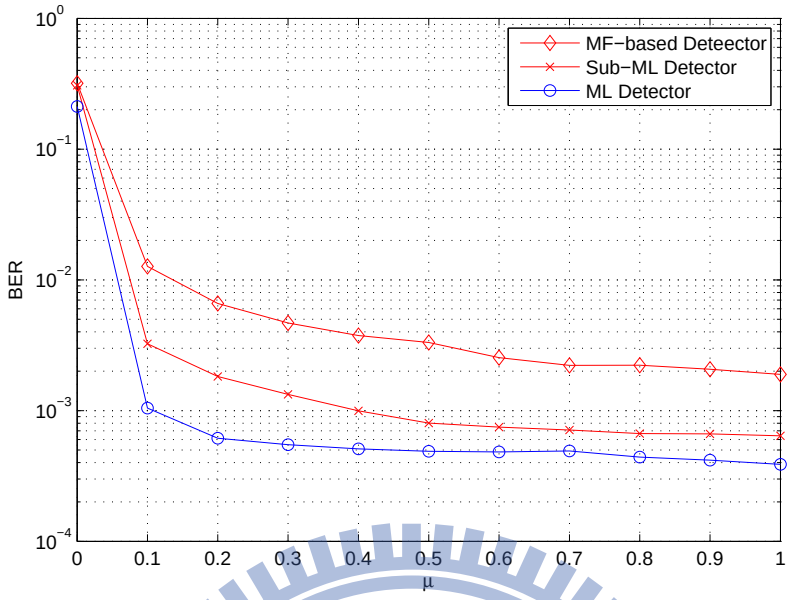

Figure 4.8: The effect of different mu (inverse of CPR) value with different detectors on BER performance.

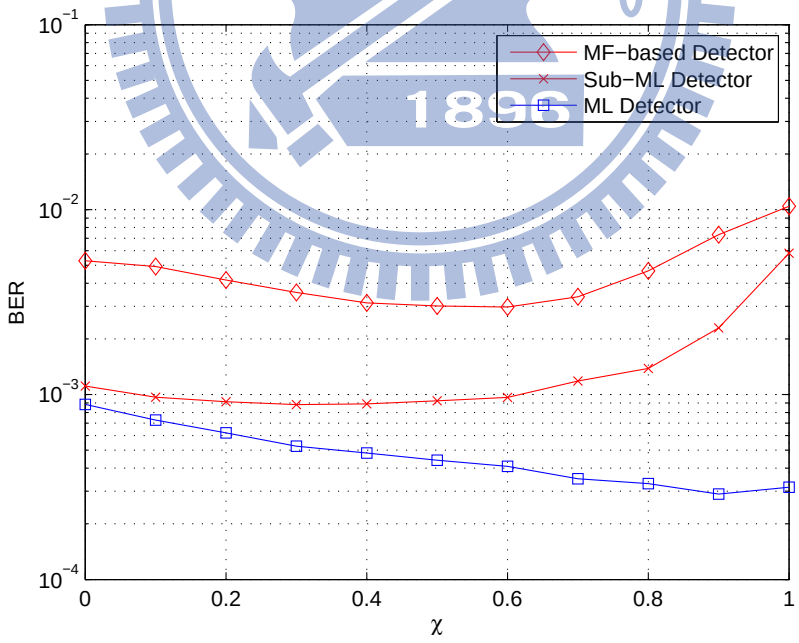

Figure 4.9: The effect of different chi (inverse of XPR) value with different detectors on BER performance.

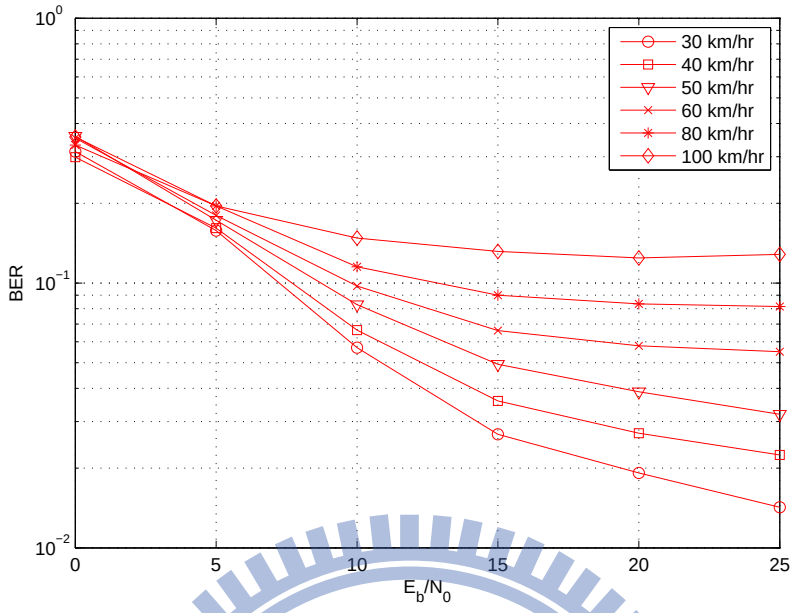

Figure 4.10: BER performance of decision-directed channel estimation method with MF-based detector in DPSC channel under different mobile velocity.

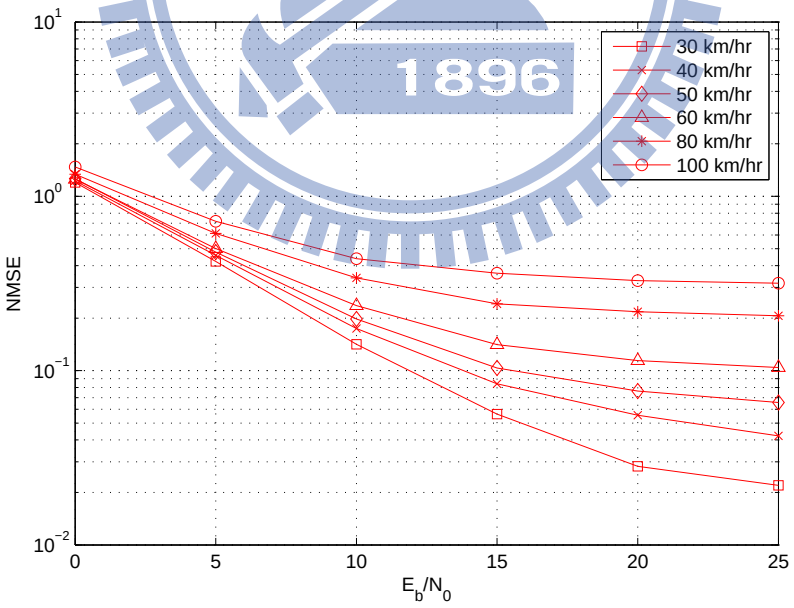

Figure 4.11: NMSE performance of decision-directed channel estimation method with MF-based detector in DPSC channel under different mobile velocity.

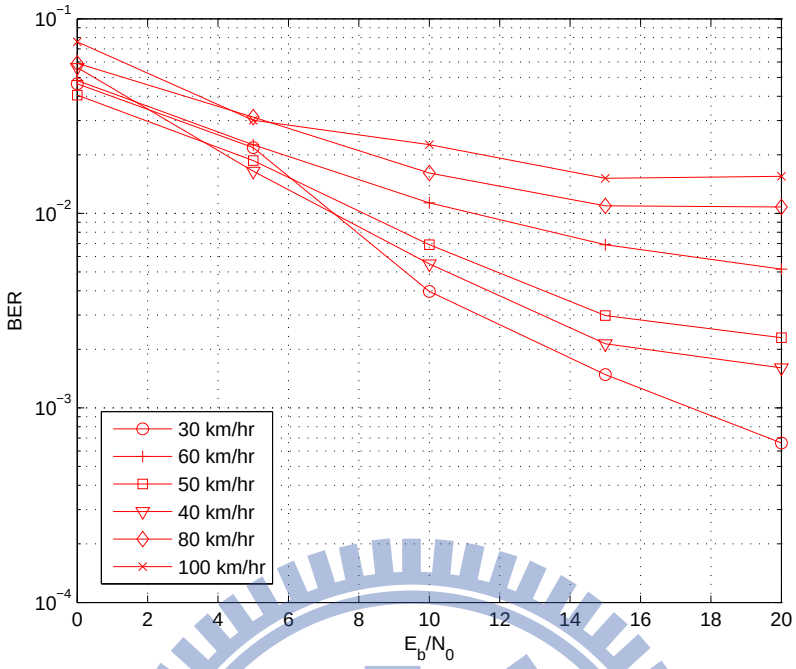

Figure 4.12: BER performance of decision-directed channel estimation method with low complexity ML detector in DPSC channel under different mobile velocity.

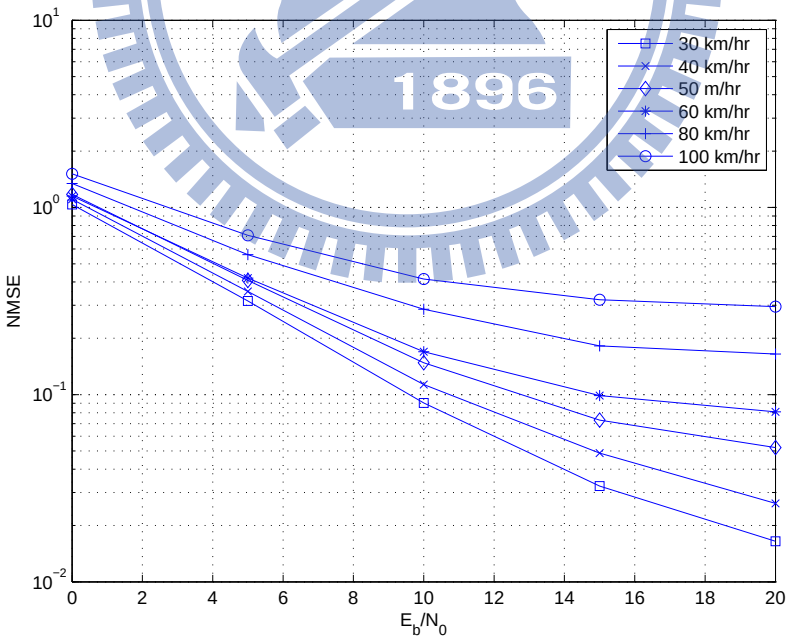

Figure 4.13: NMSE performance of decision-directed channel estimation method with low complexity ML detector in DPSC channel under different mobile velocity.

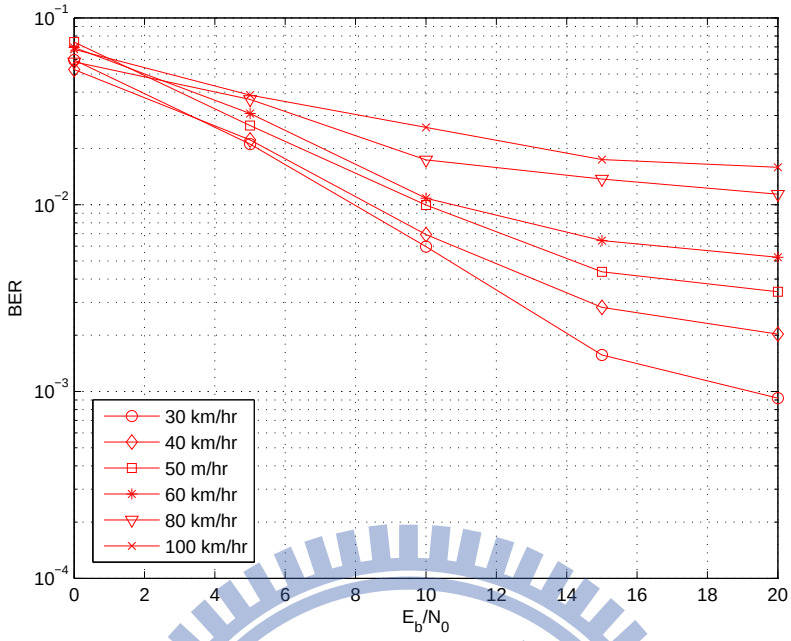

Figure 4.14: BER performance of decision-directed channel estimation method with ML detector in DPSC channel under different mobile velocity.

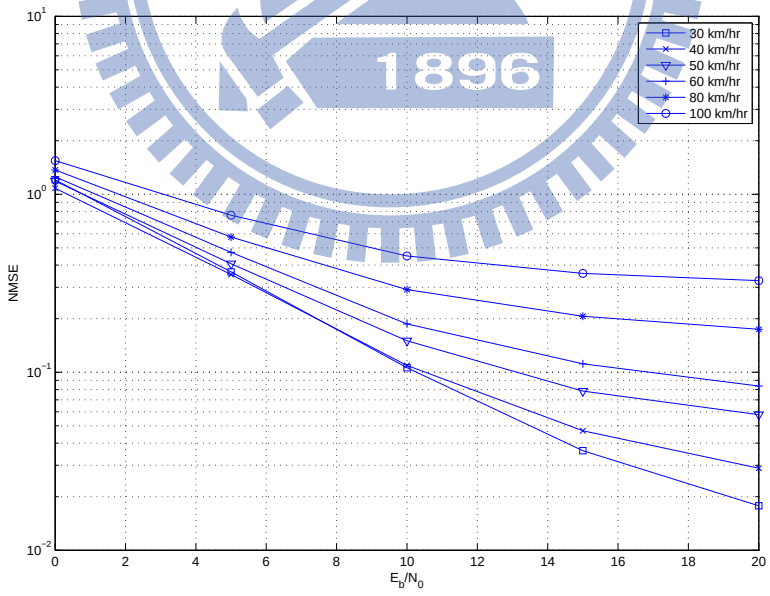

Figure 4.15: NMSE performance of decision-directed channel estimation method with ML detector in DPSC channel under different mobile velocity.

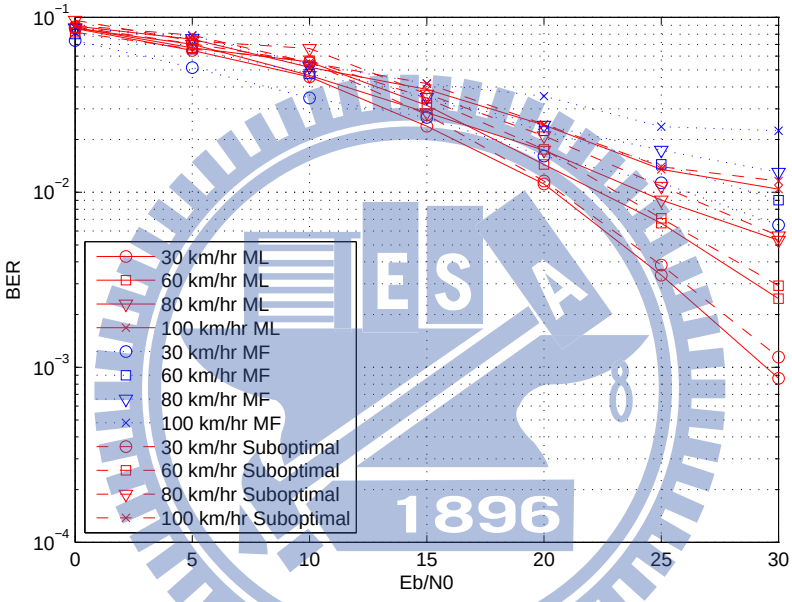

Figure 4.16: BER performance of superimposed channel estimation method based on three detectors in DPSC under different mobile velocity.

Chapter 5

Space-Time Block-Coded Spatial Modulation (STBC-SM) System

5.1 STBC-SM System

Conventional space-time block codes (STBCs) offer an excellent way to exploit the potential of MIMO systems because of the improvement of transmission reliability, obtaining both diversity and coding gain. Redundant copies of the data stream transmitted through multiple transmit antennas via STBC. As a result, different copies of the data are received and hence can provide the more reliable information. Moreover, STBC schemes are simple to implement and decode. However, the symbol rate of unitary STBCs is upper-bounded by 1 symbol per channel use. Therefore, space-time block-coded SM (STBC-SM) system is introduced to improve the spectral efficiency of conventional STBCs [28].

In the STBC-SM scheme, both STBC symbols and the indices of the transmit antennas by which these symbols are transmitted carry information. The famous STBC proposed by Alamouti [4] suggests that the system transmits two symbols, drawn from the constellation, by the two transmit antennas respectively at a time. During the first time slot, the symbols x_1 and x_2 are simultaneously transmitted by the first and second transmit antennas, respectively, then, in the next time slot, $-x_2^*$ and x_1^* are transmitted

by the respective transmit antennas. In other words, the codeword is given by

$$\mathbf{X} = [\mathbf{x}_1 \ \mathbf{x}_2] = \begin{bmatrix} x_1 & -x_2^* \\ x_2 & x_1^* \end{bmatrix}. \tag{5.1}$$

The above Alamouti codeword matrix is extended to the antenna domain for the STBC-SM system where the selection of two out of N_T antennas to transmit the two symbols introduce additional carried information. The spectral efficiency is shown to be superior to the conventional STBC or SM system in [28]. We first give an example of STBC-SM systems in the following [28].

Consider a MIMO system with four transmit antennas ($N_T = 4$), a STBC code ξ is designed to be of the following form:

$$\xi_1 = \{\mathbf{X}_{11}, \mathbf{X}_{12}\} = \left\{ \begin{bmatrix} x_1 & x_2 & 0 & 0 \\ -x_2^* & x_1^* & 0 & 0 \end{bmatrix}^T, \begin{bmatrix} 0 & 0 & x_1 & x_2 \\ 0 & 0 & -x_2^* & x_1^* \end{bmatrix}^T \right\},$$

$$\xi_2 = \{\mathbf{X}_{21}, \mathbf{X}_{22}\} = \left\{ \begin{bmatrix} 0 & x_1 & x_2 & 0 \\ 0 & -x_2^* & x_1^* & 0 \end{bmatrix}^T, \begin{bmatrix} x_2 & 0 & 0 & x_1 \\ x_1^* & 0 & 0 & -x_2^* \end{bmatrix}^T \right\} e^{j\theta}. \tag{5.2}$$

where the codebooks ξ_1 and ξ_2 contains two codewords $\mathbf{X}_{ij}$, $j = 1, 2$ that do not interfere with each other. A codebook is constructed by grouping a codewords satisfying $\mathbf{X}_{ij}^H \mathbf{X}_{ik} = \mathbf{0}_{2\times 2}$, $j, k = 1, 2$, $j \neq k$, and θ is a rotation angle to be optimized for a given modulation scheme. With this STBC-SM codebook design, coding gain and diversity gain of the scheme can be maximized. A mapping rule of this example with BPSK modulation symbols is given in Table 5.1.

When there are more than two codebooks, multiple rotation angles shall be implemented. The optimization of these rotation angles in the STBS-SM system is done by maximizing the minimum distance in the code. For detail, see [28].

Noted that the number of transmit antennas in the STBC-SM scheme needs not be an integer power of 2 as is restricted in SM scheme and thus provides design flexibility. A design procedure to generalize STBC-SM system to N_T antennas is given in the following:

Table 5.1: STBC-SM mapping table for 2 bits/transmission

	Antenna Position	Input Bits	Transmit Matrix		Antenna Position	Input Bits	Transmit Matrix
ξ_1	ℓ_1	0000	$\begin{bmatrix} 1 & 1 & 0 & 0 \\ -1 & 1 & 0 & 0 \end{bmatrix}^T$	ξ_2	ℓ_3	1000	$\begin{bmatrix} 0 & 1 & 1 & 0 \\ 0 & -1 & 1 & 0 \end{bmatrix}^T e^{j\theta}$
		0001	$\begin{bmatrix} 1 & -1 & 0 & 0 \\ 1 & 1 & 0 & 0 \end{bmatrix}^T$			1001	$\begin{bmatrix} 0 & 1 & -1 & 0 \\ 0 & 1 & 1 & 0 \end{bmatrix}^T e^{j\theta}$
		0010	$\begin{bmatrix} -1 & 1 & 0 & 0 \\ -1 & -1 & 0 & 0 \end{bmatrix}^T$			1010	$\begin{bmatrix} 0 & -1 & 1 & 0 \\ 0 & -1 & -1 & 0 \end{bmatrix}^T e^{j\theta}$
		0011	$\begin{bmatrix} -1 & -1 & 0 & 0 \\ 1 & -1 & 0 & 0 \end{bmatrix}^T$			1011	$\begin{bmatrix} 0 & -1 & -1 & 0 \\ 0 & 1 & -1 & 0 \end{bmatrix}^T e^{j\theta}$
	ℓ_2	0100	$\begin{bmatrix} 0 & 0 & 1 & 1 \\ 0 & 0 & -1 & 1 \end{bmatrix}^T$		ℓ_4	1100	$\begin{bmatrix} 1 & 0 & 0 & 1 \\ 1 & 0 & 0 & -1 \end{bmatrix}^T e^{j\theta}$
		0101	$\begin{bmatrix} 0 & 0 & 1 & -1 \\ 0 & 0 & 1 & 1 \end{bmatrix}^T$			1101	$\begin{bmatrix} -1 & 0 & 0 & 1 \\ 1 & 0 & 0 & 1 \end{bmatrix}^T e^{j\theta}$
		0110	$\begin{bmatrix} 0 & 0 & -1 & 1 \\ 0 & 0 & -1 & -1 \end{bmatrix}^T$			1110	$\begin{bmatrix} 1 & 0 & 0 & -1 \\ -1 & 0 & 0 & -1 \end{bmatrix}^T e^{j\theta}$
		0111	$\begin{bmatrix} 0 & 0 & -1 & -1 \\ 0 & 0 & 1 & -1 \end{bmatrix}^T$			1111	$\begin{bmatrix} -1 & 0 & 0 & -1 \\ -1 & 0 & 0 & 1 \end{bmatrix}^T e^{j\theta}$

Step 1: Find the number of possible combinations of two out of N_T transmit antennas. This number $c = \lfloor \binom{N_T}{2} \rfloor_{2^i}$, where i is a positive integer, should be a power of 2 to carry information bits by antenna selection.

Step 2: To make codewords in i codebook do not interfere with each other, their nonzero rows have to be nonoverlapping. Therefore, we can calculate the number of codewords in a codebook and total number of codebooks to be $a = \lfloor \frac{N_T}{2} \rfloor$ and $n = \lceil \frac{c}{a} \rceil$, respectively.

Step 3: Construct the STBC-SM codewords starting from ξ_1 which contains a non-interfering codewords as

$$\xi_1 = \{[\mathbf{X}\ \mathbf{0}_{2\times(N_T-2)}]^T, [\mathbf{0}_{2\times 2}\ \mathbf{X}\ \mathbf{0}_{2\times(N_T-4)}]^T, \cdots, [\mathbf{0}_{2\times 2(a-1)}\ \mathbf{X}\ \mathbf{0}_{2\times(N_T-2a)}]^T\}, \quad (5.3)$$

where $\mathbf{X}$ is defined as (5.1). The other codebooks, $\xi_i,\ 2 \leq i \leq n$, are created sequentially in a similar manner, where every codebook ξ_i should contain non-interfering codewords of different transmit antenna combinations and must be composed of codewords that were never used in the previous codebooks $\xi_j,\ j \leq i$.

Step 4: Determine the optimal θ_i of each codebook ξ_i by maximizing the minimum distance where $i = 1, \cdots, n$. Code $\xi = \{\xi_1, \xi_2, \cdots, n\}$ is determined.

Since there are c antenna combinations, the spectral efficiency of STBC-SM is

$$m = \frac{1}{2}\log_2 c + \log_2 M \text{ [bits/s/Hz]}, \tag{5.4}$$

where the factor $\frac{1}{2}$ is due to the normalization by the block size $B = 2$. With codeword $\mathbf{X}_\xi(k)$ drawn from this determined code, the received signal at time k can be denoted as

$$\mathbf{Y}(k) = \mathbf{H}(k)\mathbf{X}_\xi(k) + \mathbf{Z}(k), \tag{5.5}$$

where $\mathbf{X}_\xi(k)$ is an $N_T \times 2$ STBC-SM codeword matrix. While the conventional ML detector needs an exhaustive search over cM^2 metrices, i.e.,

$$\hat{\mathbf{X}}_\xi(k) = \arg\min_{\mathbf{X}_\xi \in \xi} \|\mathbf{Y}(k) - \mathbf{H}(k)\mathbf{X}_\xi\|^2, \tag{5.6}$$

the unitary property of Alamouti code suggests a simpler ML detector. Specifically, the received signal can be replaced by a $2N_R \times 1$ vector [4]

$$\mathbf{y}(k) = \mathcal{H}_\xi(k) \begin{bmatrix} x_1(k) \\ x_2(k) \end{bmatrix} + \mathbf{z}(k), \tag{5.7}$$

where $\mathcal{H}_\xi(k)$ is the $2N_R \times 2$ equivalent channel matrix corresponding to the different realizations of STBC-SM codewords. In the case of $N_T = 4$, there are $c = 4$ possible

realizations for $\mathcal{H}_\xi$,

$$\mathcal{H}_{\ell_1} = \begin{bmatrix} h_{1,1} & h_{1,2} \\ h_{1,2}^* & -h_{1,1}^* \\ \vdots & \vdots \\ h_{N_R,1} & h_{N_R,2} \\ h_{N_R,2}^* & -h_{N_R,1}^* \end{bmatrix}, \quad \mathcal{H}_{\ell_2} = \begin{bmatrix} h_{1,3} & h_{1,4} \\ h_{1,4}^* & -h_{1,3}^* \\ \vdots & \vdots \\ h_{N_R,3} & h_{N_R,4} \\ h_{N_R,4}^* & -h_{N_R,3}^* \end{bmatrix}, \tag{5.8}$$

$$\mathcal{H}_{\ell_3} = \begin{bmatrix} h_{1,2}\varphi & h_{1,3}\varphi \\ h_{1,3}^*\varphi & -h_{1,2}^*\varphi \\ \vdots & \vdots \\ h_{N_R,2}\varphi & h_{N_R,3}\varphi \\ h_{N_R,3}^*\varphi & -h_{N_R,2}^*\varphi \end{bmatrix}, \mathcal{H}_{\ell_4} = \begin{bmatrix} h_{1,4}\varphi & h_{1,1}\varphi \\ h_{1,1}^*\varphi & -h_{1,4}^*\varphi \\ \vdots & \vdots \\ h_{N_R,4} & h_{N_R,1} \\ h_{N_R,1}^*\varphi & -h_{N_R,4}^*\varphi \end{bmatrix},$$

where $\varphi = e^{j\theta}$ and time index k is neglected for the moment. The ML detector (5.9) can be simplified and decoupled into two independent ML symbol detectors due to the column-orthogonality in every $\mathcal{H}_{\ell_i}$, i.e,

$$(\hat{\ell}_i, \hat{x}_{j,\ell_i}(k)) = \arg \min_{\ell_i, x_j \in \gamma} \|\mathbf{y}(k) - \mathbf{h}_{\ell_i,j}(k) x_j\|^2, \ j = 1, 2. \tag{5.9}$$

5.2 Differential STBC-SM Scheme

Differential space-time modulation (DSTM) has received much attention recent by, since it not only avoids MIMO channel estimation but also can achieve considerably high spatial diversity gain. In order to realize DSTM, the data information needs to be first encoded into differential space-time block codes (DSTBCs). In general, DSTBC is designed to be unitary to simplify the transceiver [34].

In the thesis, we propose a differential STBC-SM system which dose not need CSI knowledge at the receiver and thus outperforms STBC-SM in the presence of channel estimation error. With the need that the DSTBCs should be unitary, it necessitates us to modify the non-unitary Alamouti code-based STBC-SM codewords introduced in the previous section.

Due to the fact that for an N_T-transmit-antenna STBC-SM system, only two transmit antennas are selected to transmit symbols and the rest of the antennas are inactive, we

let the number of transmit antennas be even 2 and extend the STBC-SM codeword matrix to $N_T \times N_T$ with a procedure given later. We recall the $N_T = 4$ case as an example, the STBC-SM codeword

$$\mathbf{X}_\xi = \begin{bmatrix} x_1 & x_2 & 0 & 0 \\ -x_2^* & x_1^* & 0 & 0 \end{bmatrix}^T \tag{5.10}$$

can be extended to an unitary matrix by extending the block size $B = 4$ and letting the unused antennas to transmit additional symbols in time instants 3 and 4. The corresponding DSTBC codeword matrix becomes

$$\mathbf{X}_D = \begin{bmatrix} x_1 & x_2 & 0 & 0 \\ -x_2^* & x_1^* & 0 & 0 \\ 0 & 0 & x_3 & x_4 \\ 0 & 0 & -x_4^* & x_3^* \end{bmatrix}. \tag{5.11}$$

Similar procedures generalized to other value of N_T is depicted as follows:

Step 1: Each codeword designed for the N_T-transmit antenna STBC-SM system is taken as the first two columns of a DSTBC codeword matrix.

Step 2: To achieve the unitary property, the available transmit antennas at the third and fourth time cannot include the transmit antennas used in the previous tow instants. Therefore, the third and fourth columns (negleting the rows in which the first two columns have nonzero elements) are designed to be the codewords of $(N_T - 2)$-antenna STBC-SM system.

Step 3: Similar process is done to the fifth and sixth columns and the remaining columns by neglecting the occupied rows by the previous steps until all columns are considered.

Since we produce $c_k = \left\lfloor \binom{N_T - 2(k-1)}{2} \right\rfloor_{2^i}$ possible combinations at each step k, the spectral efficiency of the proposed DSTBC-SM system is

$$m = \frac{1}{N_T}(\log_2 c_1 + \log_2 c_2 + \cdots + \log_2 c_{\frac{N_T}{2}}) + \log_2 M \text{ [bits/s/Hz]} \tag{5.12}$$

which is smaller than that of STBC-SM system (5.9).

Let each symbol x_i be taken from a unimodular $\in \xi_D$ constellation with energy E_x (e.g. M-PSK, M-QAM, etc). For each codeword $\mathbf{X}_D$, it satisfies

$$\mathbf{X}_D \mathbf{X}_D^H = 2E_x \mathbf{I}_{N_T}, \tag{5.13}$$

where ξ_D is the code constructed via the procedure and is of cardinality $\prod_{k=1}^{\frac{N_T}{2}} c_k$. An identity matrix which dose not contain any information is sent to initialize the transmission, i.e, $\mathbf{V}_D(0) = \mathbf{I}_{N_T}$. By mapping information bits to a DSTBC-SM codeword, the differential encoded codeword matrix of the kth block becomes

$$\mathbf{V}_D(k) = \tilde{\mathbf{V}}_D(k-1)\mathbf{X}_D, \ k \geq 2 \tag{5.14}$$

where

$$\tilde{\mathbf{V}}_D(k-1) = \frac{1}{\sqrt{2E_x}} \mathbf{V}_D(k-1) \tag{5.15}$$

denotes the normalized version of $\tilde{\mathbf{V}}_D(k-1)$ to ensure constant transmission power, i.e., $\tilde{\mathbf{V}}_D(k-1)\tilde{\mathbf{V}}_D^H(k-1) = \mathbf{I}_{N_T}$.

As a result, the received signals at $(k-1)$- and kth block are respectively

$$\mathbf{Y}(k-1) = \mathbf{H}(k-1)\mathbf{V}_D(k-1) + \mathbf{Z}(k-1), \tag{5.16}$$

$$\mathbf{Y}(k) = \mathbf{H}(k)\mathbf{V}_D(k) + \mathbf{Z}(k). \tag{5.17}$$

For slow time-varying channel, the channel matrices at two consecutive block times are similar, hence $\mathbf{H}(k-1) \cong \mathbf{H}(k)$. The optimal non-coherent detector can be

$$\hat{\mathbf{X}}_D(k) = \arg \min_{\mathbf{X}_D \in \xi_D} \|\mathbf{Y}(k) - \frac{1}{\sqrt{2E_x}} \mathbf{Y}(k-1)\mathbf{X}_D\|^2. \tag{5.18}$$

In addition, due to the unitary structure of Alamouti code, the transmit data symbols can be estimated individually via the similar approach discussed in (5.8)–(5.7). Therefore, the complexity of the optimal non-coherent detector is further reduced.

5.3 Simulation Results

The performances of the proposed DSTBC-SM are given in this section. In Figure 5.1, we compare the performance of STBC-SM and DSTBC-SM. The transmit and

receive antennas are set to 4, and the slow-tim varying channel is generated by Jake's model the same as in previous Chapters. The performance of DSTBC-SM with QPSK modulation under the mobile velocity of 40 km/hr outperforms STBC-SM with LS channel estimation error due to the fact that the differential design dose not need CSI at the receiver and can thus avoid the estimation error effect. We also investigate the DSTBC-SM performance under different mobile velocity in Figure 5.2, and it can be seen that the performance degrades with higher mobile velocity.

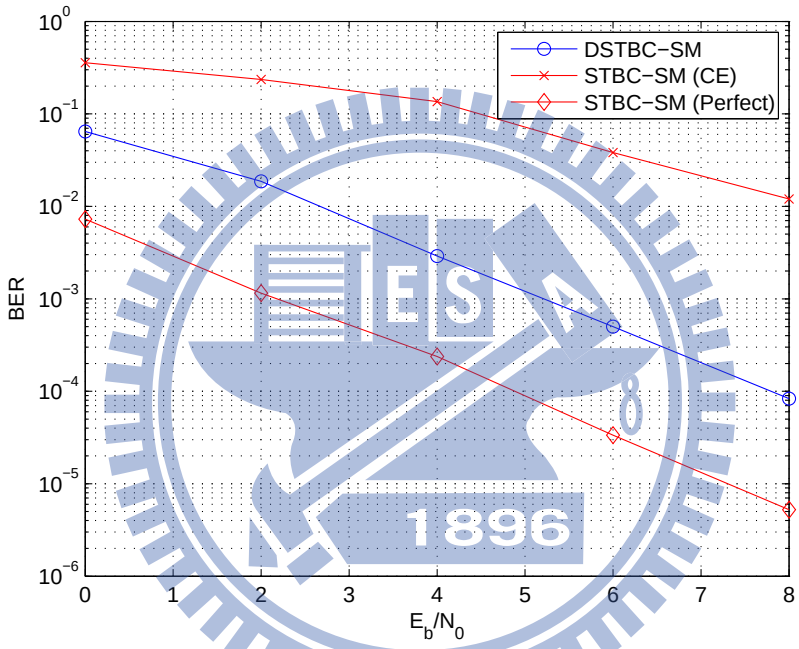

Figure 5.1: Comparison of BER performance for STBC-SM with perfect CSI, DSTBC-SM and STBC-SM with channel estimation error.

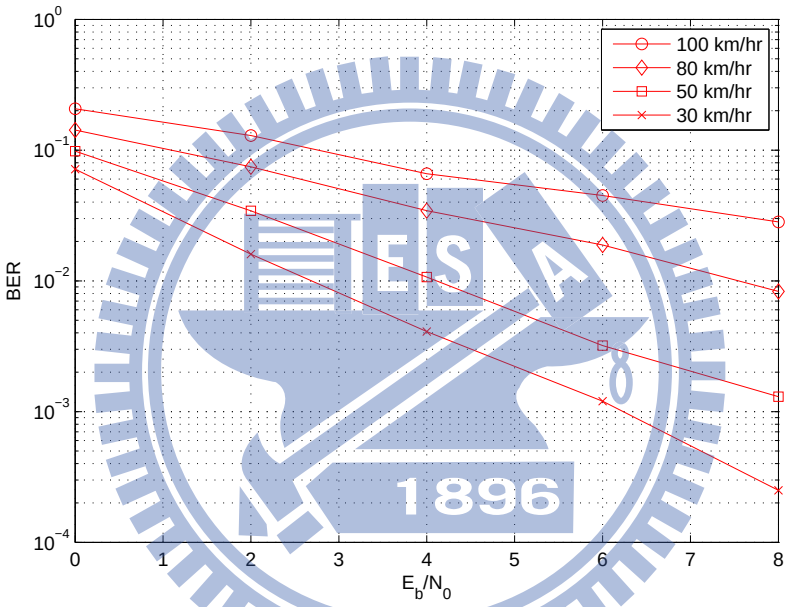

Figure 5.2: BER performance of DSTBC-SM for different mobile velocity.

Chapter 6

Conclusion

Several issues associated with SM systems are investigated in this thesis. We first propose two channel estimators for time-varying SM channels. The decision-directed estimator gives good error-rate performance when SNR is not too high but exhibits error floor in high SNR regime. To overcome the error propagation effect, we propose a superimposed pilot-aided estimator which not only outperforms the decision-directed method but reduce the pilot overhead.

New SM schemes for dual-polarized antenna arrays are then presented, along with a modified channel estimator which takes into account the spatial correlations. The corresponding signal mapping and MF-based and ML detection techniques are proposed. We also suggest a suboptimal low-complexity detector which achieves near-ML performance.

Looking into the depolarization effect on the performance of these detectors, we find that considerable performance degradation incurs when the CPR value is small. On the other hand, large XPR values cause performance loss on the MF-based and suboptimal detectors but have little or no influence on the ML detector's performance.

We also propose a differential STBC-SM scheme to relieve the burden of channel estimation requirement. The simulation result shows that it performs well in slow time-varying environments and outperforms the conventional STBC-SM with imperfect CSI knowledge.

Detailed studies on the feasibilities of various SM systems, including cost, complexity

and implementation losses have to be performed before the SM technology becomes a realistic design option. As has been mentioned, the spatial channels have to be dissimilar to a certain extent for the receiver to resolve the transmit antenna indices. We think there must be ways to make the equivalent MIMO subchannels as dissimilar as possible by proper signal design.

Finally, we notice that the SM scheme has recently been applied for high speed LED (array) communications where optical on-off keying is used. To enhance the throughput of such optical communication systems, higher-order modulations like PPM or PAM can be employed. In an indoor environment where multiple optical sources coexist, optical interference must be considered and the associated interference-insensitive detection scheme has to be developed if LED communication systems are to become practical.

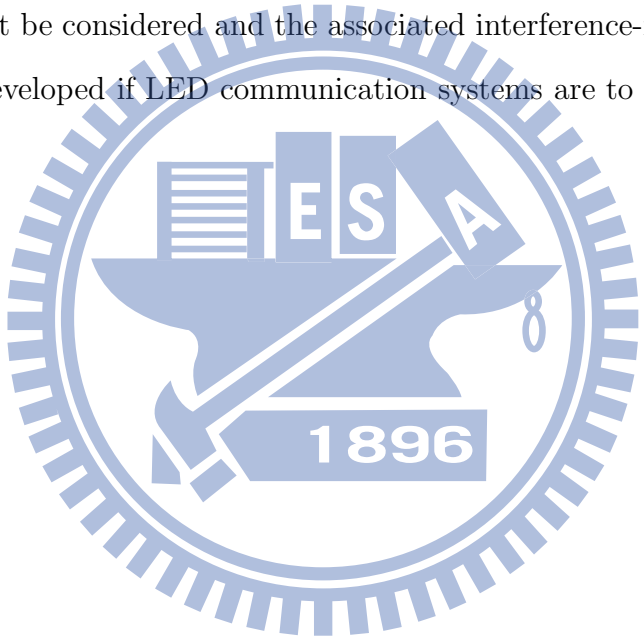

Appendix A

In order to find a set of basis for the null space matrix that can be used to separate superimposed pilots from data matrix, the choices of basis need to be satisfy a specific form. Since each column of the data matrix $\mathbf{X}(k)$ only has one nonzero element, it is not complicated to find the basis of its null space. We give the algorithm to solve this issue as follows.

Let one data matrix $\mathbf{X}$ of size $N_T \times B$ be

$$\mathbf{X} = \begin{bmatrix} x_{1,1} & x_{1,2} & \cdots & x_{1,B} \\ x_{2,1} & x_{2,2} & \cdots & x_{2,B} \\ \vdots & \vdots & \cdots & \vdots \\ x_{N_T,1} & x_{N_T,2} & \cdots & x_{N_T,B} \end{bmatrix} \tag{1}$$

, and define the $B \times M$ matrix $\mathbf{N}_x$ which consists of the null space basis of $\mathbf{X}$ and $M = Nullity(\mathbf{X})$,

$$\mathbf{N}_x = \begin{bmatrix} n_{x1,1} & n_{x1,2} & \cdots & n_{x1,M} \\ n_{x2,1} & n_{x2,2} & \cdots & {}_{x2,M} \\ \vdots & \vdots & \cdots & \vdots \\ n_{xB,1} & n_{xB,2} & \cdots & n_{xB,M} \end{bmatrix}. \tag{2}$$

These two matrices satisfy the condition that $\mathbf{X}\mathbf{N}_x = \mathbf{0}$. This is equal to solve a homogeneous system of linear equations:

$$n_{x1,j}x_{i,1} + n_{x2,j}x_{i,2} + \cdots + n_{xB,j}x_{i,B} = 0,\ j = 1, \cdots, M \tag{3}$$

where the bases are found by the rows of matrix $\mathbf{X}$ whose nonzero elements are larger than one. For each equation, we set the second variable with nonzero coefficient to 1 and solve the value of the first variable by setting other variables to zero and thus we can get one basis of the null space. Then the second variable with nonzero coefficient is set

to 0 and the third nonzero coefficient is set to 1 and solve the value of the first variable to get another basis. The rest can be done by the same manner until all coefficients are solved in one equation. By this way, we can get M basis of the null space for matrix $\mathbf{X}$ to form $\mathbf{N}_x$.

For example, when a 4×4 BPSK data matrix is used,

$$\mathbf{X} = \begin{bmatrix} 1 & 1 & -1 & 0 \\ 0 & 0 & 0 & 1 \\ 0 & 0 & 0 & 0 \\ 0 & 0 & 0 & 0 \end{bmatrix}, \tag{4}$$

the corresponding $\mathbf{N}_x$ is

$$\mathbf{N}_x = \begin{bmatrix} -1 & 1 \\ 1 & 0 \\ 0 & 1 \\ 0 & 0 \end{bmatrix}. \tag{5}$$

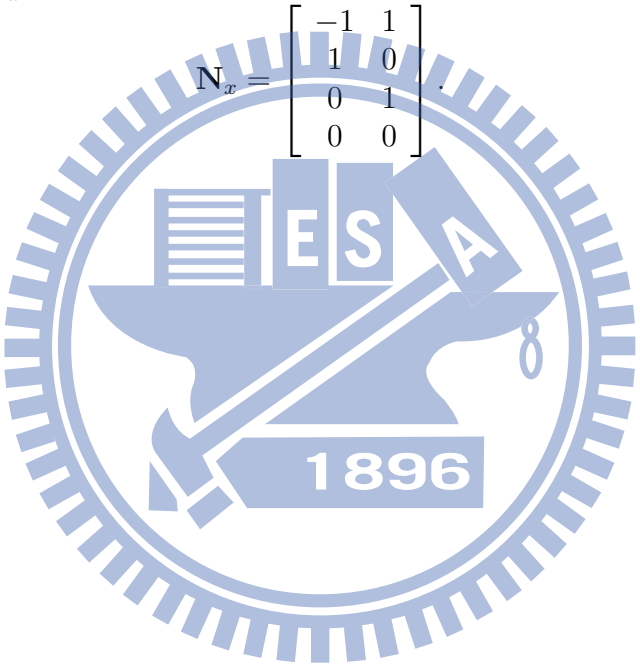

Bibliography

[1] D. Tse and P. Viswanath, *Fundamentals of Wireless Communication*, Cambridge University Press, 2005.

[2] İ. E. Telatar, "Capacity of multi-antenna Gaussian channels," *Eur. Trans. Telecommun.*, vol. 10, no. 6, pp. 585–595, Nov., 1999.

[3] E. Biglieri, R. Calderbank, A. Constantinides, A. Goldsmith, A. Paulraj, and H. V. Poor, *MIMO Wireless Communications.*, Cambridge University Press, 2007.

[4] A. Paulraj, R. Nabar, and D. Gore, *Introduction to Space-Time Wireless Communications*, Cambridge University Press, 2003.

[5] V. Tarokh, N. Seshadri, and A. Calderbank, "Space-time codes for high data rate wireless communication: Performance criterion and code construction," *IEE Trans. Inf. Theory*, vol. 44, no. 2, pp. 744–765, Mar. 1998.

[6] G. J. Foschini, "Layered space-time architecture for wireless communication in a fading environment when using multi-element antennas," *Bell Labs Tech. J.*, vol. 1, no. 2, pp. 41–59, Sep. 1996.

[7] R. Meslsh, H. Haas, S. Sinanović, C. W. Ahn, and S. Yun, "Spatial modulation," *IEEE Trans. Veh. Technol.*, vol. 57, no. 4, pp. 2228–2241, Jul. 2008.

[8] M. D. Renzo and H. Haas, "Performance comparison of different spatial modulation schemes in correlated fading channels," in *Proc. IEEE ICC 2010*, pp. 1–6, May 2010.

[9] M. D. Renzo, H. Haas, and P. M. Grant, "Spatial modulation for multiple-antenna wireless system: a survey," *IEEE Commun. Mag.*, vol. 49, no. 12, pp. 182–191, Dec. 2011.

[10] J. Jeganathan, A. Ghrayeb, and L. Szczecinski, "Space shift keying modulation for MIMO Channels," *IEEE Commun. Mag.*, vol. 8, no. 7, pp. 3692–3703, Jul. 2009.

[11] F. A. Prisecaru and H. Hass. (2007) Mutual information and capacity of spatial modulation system., school of Engineering and Science Jacobs University, Germeny. [Online]. Available: http://www.eecs.iu-bremen.de/archive/bsc-2007/prisecaru.pdf

[12] J. Jeganathan, A. Ghrayeb, and L. Szczecinski, "Spatial modulation: Optimal detection and performance analysis," *IEEE Commun. Lett.*, vol. 12, no. 8, pp. 545–547, Aug. 2008.

[13] M. D. Renzo, R. Meslsh, and H. Haas, "Sphere decoding for spatial modulation," in *Proc. IEEE ICC 2011*, pp. 1–6, Jun. 2011.

[14] M. Biguesh and A. B. Gershman, "Training-based MIMO channel estimation: A study of estimator tradeoffs and optimal training signals," *IEEE Trans. Signal Process.*, vol. 54, no. 3, pp. 884–893, Mar. 2006.

[15] P. Zhang, I. Dey, S. Sugiura and S. Chen, "Semi-blind adaptive space-time shift keying systems based on iterative channel estimation and data detection," *IEEE VTC 2011-Spring*, pp. 1–5, May 2011.

[16] S. Sugiura, C. Xu, S. X. Ng, and L. Hanzo, "Reduced-complexity coherent versus non-coherent QAM-aided space-time shift keying," *IEEE Trans. Commun.*, vol. 59, no. 11, pp. 3090–3101, Nov. 2011.

[17] T. Weichse and P. Eggers, "Simultaneous characterization of polarization matrix components in pico cells," *IEEE VTC 1999-Fall*, vol. 3, pp. 1361–1365, Sep. 1999.

[18] A. S. Y. Poon and D. N. C. Tse, "Degree-of-freedom gain from using polarimetric antenna elements," *IEEE Trans. Inf. Theory*, vol. 57, no. 9, pp. 5695–5709, Sep. 2011.

[19] C. Oestges, B. Clerckx, M. Guillaud, and M. Debbah, "Dual-polarized wireless communications: From propagation models to system performance evaluation," *IEEE Trans. Commun.*, vol. 7, no. 10, pp. 4019–4031, Oct. 2008.

[20] C. Oestges, V. Erceg, and A. J. Paulraj, "Propagation modeling of MIMO multipolarized fixed wireless channels," *IEEE Trans. Veh. Technol.*, vol. 53, no. 4, pp. 644–654, May 2004.

[21] M. Coldrey, "Modeling and capacity of polarized MIMO channel," *IEEE VTC-Spring*, pp. 440–444, May 2008.

[22] C. Degen and W. Keusgen, "Performance evaluation of MIMO systems using dual-polarized antennas," in *Proc. IEEE ICT 2003*, vol. 2, pp. 1520–1525, Feb. 2003.

[23] J. P. Kermoal, L. Schumacher, K. I. Pedersen, P. E. Mogensen, and F. Frederiksen, "A stochastic MIMO radio channel model with experimental validation," *IEEE J. Sel. Areas Commun.*, vol. 20, no. 6, pp. 1211–1226, Aug. 2002.

[24] W. Weichselberger, M. Herdin, H. Özcelik, and E. Bonek, "A stochastic MIMO channel model with joint correlation of both link ends," *IEEE Trans. Commun.*, vol. 5, no. 1, pp. 90–100, Jan. 2006.

[25] A. M. Sayeed, "Deconstructing multiantenna fading channels," *IEEE Trans. Signal Process.*, vol. 50, no. 10, pp. 2563–2579, Oct. 2002.

[26] W. Weichselberger, M. Herdin, H. Özcelik, and E. Bonek, "A stochastic MIMO channel model with joint correlation of both link ends," *IEEE Trans. Commun.*, vol. 5, no. 1, pp. 90–100, Jan. 2006.

[27] Y. C. Chen and Y. T. Su, "MIMO channel estimation in correlated fading environments," *IEEE Trans. Commun.*, vol. 9, no. 3, pp. 1108–1119, Mar. 2010.

[28] E. Başar, Ü. Aygölü, E. Panayırcı, and H. V. Poor, "Space-time block coded spatial modulation," *IEEE Trans. Commun.*, vol. 59, no. 3, pp. 823-832, Mar. 2011.

[29] S. M. Kay, *Fundamentals of Statistical Signal Processing: Estimation Theory*, Prentice-Hall PTR, 1998.

[30] G. Taricco and E. Biglieri, "Space-time decoding with imperfect channel estimation," *IEEE Trans. Inf. Theory*, vol. 48, no. 2, pp. 359–383, Feb. 2002.

[31] L. Zheng and D. N. C. Tse, "Communication on the Grassman manifold: A geometric approach to the noncoherent multiple-antenna channel," *IEEE Trans. Inf. Theory*, vol. 48, no. 2, pp. 359–383, Feb. 2002.

[32] F. B. Gross, "New approximation to ..0 and ..1 Bessel functions," *IEEE Trans. Antennas Propag.*, vol. 43, no. 8, pp. 904–907, Aug. 1995.

[33] A. D. R. McQuarrie and C.-L. Tsai, *Regression and Time Series Model Selection. World Scientific*, World Scientific, 1998.

[34] Tarokh V and Jafarkhani H, "A differential detection scheme for transmit diversity," *IEEE J Sel. Areas Commun.*, vol. 18, pp. 1169–1174 , Jul. 2000.

[35] W. C. Jakes, *Microwave Mobile Communications*, New York: Wiley, 1974.

Autobiography

I graduated from National Chiao Tung University in Taiwan. Both my Master's and Bachelor's degrees are in Communications Engineering. From a happy middle class family, my father is a civil servant and my mother is a house wife. My brother studies EE in National Sun Yat-Sen University in Taiwan.

For the past six years, I have studied well on some courses which have given me a foundation in several areas, such as Coding Theory, Wireless Communication, and Mobile Computing. Among those courses, I am most interested in signal processing and communication systems.

During the two years of Master's degree, I did my research in "Transmission and Networking Technologies Lab", learning the advanced knowledge of communication systems with Prof. Yu T. Su. When doing research, the most valuable thing I got was the skill of how to find useful resources efficiently, and solve problems by myself.

After all, I am truly grateful to all the members of lab 811 and Prof. Yu T. Su . Without them, my life would not be so colorful.